Energy Research and Development Division
FINAL PROJECT REPORT

RENEWABLE RESOURCE MANAGEMENT AT UC SAN DIEGO

Prepared for: California Energy Commission
Prepared by: Jan Kleissl, William V. Torre, Byron Washom, UC San Diego

MARCH 2015
CEC-500-2016-027

PREPARED BY:

Primary Author(s):
Jan Kleissl, William V. Torre, Byron Washom

Center for Energy Research
University of California, San Diego.
9500 Gilman Dr.
La Jolla, CA, 92093
jkleissl@ucsd.edu

Contract Number: 500-10-043

Prepared for:

California Energy Commission

Quenby Lum
Contract Manager

Fernando Pina
Office Manager
Energy Systems Research

Laurie ten Hope
Deputy Director
ENERGY RESEARCH & DEVELOPMENT

Robert Oglesby
Executive Director

DISCLAIMER

This report was prepared as the result of work sponsored by the California Energy Commission. It does not necessarily represent the views of the Energy Commission, its employees or the State of California. The Energy Commission, the State of California, its employees, contractors and subcontractors make no warrant, express or implied, and assume no legal liability for the information in this report; nor does any party represent that the uses of this information will not infringe upon privately owned rights. This report has not been approved or disapproved by the California Energy Commission nor has the California Energy Commission passed upon the accuracy or adequacy of the information in this report.

PREFACE

The California Energy Commission Public Interest Energy Research (PIER) Program supports public interest energy research and development that will help improve the quality of life in California by bringing environmentally safe, affordable, and reliable energy services and products to the marketplace.

The PIER Program conducts public interest research, development, and demonstration (RD&D) projects to benefit California.

The PIER Program strives to conduct the most promising public interest energy research by partnering with RD&D entities, including individuals, businesses, utilities, and public or private research institutions.

PIER funding efforts are focused on the following RD&D program areas:

- Buildings End-Use Energy Efficiency
- Energy Innovations Small Grants
- Energy-Related Environmental Research
- Energy Systems Integration
- Environmentally Preferred Advanced Generation
- Industrial/Agricultural/Water End-Use Energy Efficiency
- Renewable Energy Technologies
- Transportation

Report on *Renewable Resource Management at UC San Diego* is a deliverable for the California Energy Commission contract number 500-10-043 conducted by the University of California, San Diego. The information from this project contributes to PIER's Renewable Energy Program.

When the source of a table, figure or photo is not otherwise credited, it is the work of the author of the report.

For more information about the PIER Program, please visit the Energy Commission's website at www.energy.ca.gov/research/ or contact the Energy Commission at 916-654-4878.

ABSTRACT

The use of microgrids has recently been a favored method of providing energy to local communities due to control capability, cost efficacy, and the ability to operate autonomously. In an effort to provide further microgrid efficiency, the research team at the University of California, San Diego sought to introduce several methods of renewable resource integration within their microgrid. The researchers designated a total of four primary integration objectives, which included: (1) providing accurate intra-hour forecasting for solar generation; (2) analyzing the impact of photovoltaic and electric vehicles on microgrid voltages while demonstrating the ability of integrated photovoltaic and energy storage to smooth solar variability, reduce demand charge, and capture regulation value streams; (3) facilitating the ability to identify, analyze, and comprehend the functions of the microgrid by the California Independent System Operator; and (4) showing the feasibility of a direct current linked, renewable energy electric vehicle charge port with energy storage. Each project individually provided stable and efficient means of integrating renewable energy sources into the microgrid and improved overall energy savings. Since each project was uniquely different, there were several result findings, most of which still require additional research and applicable changes to provide the best possible outcome for integration and energy savings. Through this project, the researchers at the University of California, San Diego gained a better understanding of energy integration and situational awareness related to microgrid operation.

Keywords: solar forecast, microgrid, energy storage, electric vehicle, solar power integration

Please use the following citation for this report:

Kleissl, Jan; Torre, William; Washom, Byron, 2015. *Renewable Resource Management at UC San Diego, California Energy Commission*. Publication Number: CEC-500-2016-027.

TABLE OF CONTENTS

PREFACE ..... **i**

ABSTRACT ..... **ii**

LIST OF FIGURES ..... **iv**

LIST OF TABLES ..... **v**

EXECUTIVE SUMMARY **1**

Introduction 1

Project Purpose 1

Project Results 2

Project Benefits 6

CHAPTER 1: Introduction **7**

CHAPTER 2: Hardware Deployments and Control Algorithm Development for Solar Power Integration **10**

2.1 30 kW by 30 kWh PV Integrated Energy Storage 10

2.2 125 kW by 65 kWh EV Battery Test Stand DESS 11

2.3 Renewable Energy Electric Vehicle Charging at San Diego Zoo 12

2.4 Solar Forecasting at a Utility Scale Power Plant 14

2.4.1 Sky Imagery and Inverter Power Output Data 14

2.4.2 Cloud Speed Persistence Forecast Method 16

2.4.3 Sky Imager Forecast Method 19

2.5 Microgrid Observability Test with the CAISO 21

2.5.1 Microgrid Connection to CAISO 21

2.5.2 CAISO Market Simulation of the UCSD Microgrid 24

CHAPTER 3: Distributed Energy Resource Applications **26**

3.1 Demand Charge Reduction Using Energy Storage and Forecasting 26

3.2 Battery Characterization and Use Cases for Regulation and Demand Charge Management 28

3.2.1 Battery Health Testing and Backup Power Application 28

3.2.2 Use Case Regulation Energy Management (REM) 29

3.2.3 Use Case Demand Charge Management (DCM). 30
3.3 Peak Shifting and Solar Variability Smoothing with Energy Storage 30
3.4 Operational experience of EV Charging with solar energy 32
3.5 Cumulative Impacts of High Penetration of EV Charging and Photovoltaic Generation. 35
3.6 Solar Forecast Results 38
3.6.1 Forecasting Using Ground Data without Sky Imagery 38
3.6.2 Sky Imagery Forecast Results 40
CHAPTER 4: Distributed Energy Resource Characterization and Lessons Learned .. 45
4.1 Battery Degradation and Life Expectancy 45
4.2 Battery System Charge Efficiency 46
4.3 EV Charging Costs and CO2 Emissions 47
4.4 Intra-Hour Solar Forecast Accuracy 48
CHAPTER 5: Summary and Conclusions 50
GLOSSARY 52
REFERENCES 53

LIST OF FIGURES

Figure ES-1: 48 MW Section of the Sempra US Gas & Power Copper Mountain Solar Power Plant 3
Figure ES-2: Illustration of the Cloud Speed Persistence Approach 4
Figure ES-3: Sanyo-Panasonic Energy Storage System Efficiency 5
Figure 1: Sanyo Dess System Summary 10
Figure 2: Sanyo DESS Battery System and PV Solar Panels 11
Figure 3: Smart City Renewable Energy Charging Project 13
Figure 4: 48MW Section of the Sempra US Gas and Power Copper Mountain Solar Power Plant 15
Figure 5: Satellite Photograph of the Sempra US Gas and Power CMS1 Photovoltaic Plant 16
Figure 6: Inverter Power Output Distribution 18
Figure 7: Flow Chart for Constructing Power Forecast in Copper Mountain Case Study 20

Figure 8: How Shadowmaps are Generated From Ray Tracing 21
Figure 9: User Screens Developed by Power Analytics Paladin Control System 23
Figure 10: Campus Power Network 23
Figure 11: Second Life Battery Dashboard and Real Time Phasor Diagram 24
Figure 12: Example of Control Optimization System 27
Figure 13: C/5 Capacity Test Results 28
Figure 14: Pulse Characterization Test 29
Figure 15: Regulation Energy Management (REM) Duty Cycle 29
Figure 16. Demand Charge Management (DCM) Duty Cycle 30
Figure 17: PV Intermittency Smoothing Using Energy Storage 32
Figure 18: Number of Plug-in Events 34
Figure 19: Average 24 Hour Load Profile for EV Charging 35
Figure 20: RWE Intelligent Level II EV Charger 36
Figure 21: 370 kW Roof Top PV on UCSD Hopkins Parking Structure 36
Figure 22: Minimum Voltage Deviations for the Preceding and Coinciding Intervals 37
Figure 23: Distribution of the Length of the Maximum Forecast Horizon 39
Figure 23: Distribution of Maximum Forecast Horizons 40
Figure 24: Forecast Performance 41
Figure 25: Cloud Overlay from the Total Sky Imager Over the Copper Mountain Solar Power Plant 42
Figure 26: Midday 10 Minute Forecast Performance 44
Figure 27: Degradation of Battery Capacity During Laboratory Tests 46
Figure 28. Sanyo-Panasonic Energy Storage System Efficiency 47
Figure 29: SDG&E EV-TOU2 Whole House Rate 48

LIST OF TABLES

Table 1: PEV Energy Consumption and PV Energy Production 33
Table 2: The rRMSE of the Forecast Methods that Do Not Require Sky Images 38
Table 3: Sky Imager (SI) and Persistence (P) Forecast Error 43

EXECUTIVE SUMMARY

Introduction

This report summarizes the research efforts of the University of California, San Diego (UCSD), specifically the integration of renewable resources into the energy network of the local microgrid. Integration of renewable resources does not only benefit the environment, but can also be cost effective for microgrid users. Several deployment projects including solar forecasting, energy storage, electric vehicles, and microgrid situational awareness, were developed to facilitate integration.

Project Purpose

In total there were four different methods the researchers used to facilitate renewable resource integration within the UCSD microgrid. Overall, the purpose of integration was to provide alternative means for producing stable and efficient energy, as well as energy savings.

The researcher's first attempt of integration was tested using solar forecasting. Solar forecasting of the spatiotemporal variability of solar power is critical when integrating large amounts of solar power within a microgrid network. Intra-hour solar forecasting alerts electric system operators about impending ramp events requiring adjustments in load following (adjusting power output as demand for electricity fluctuates throughout the day) or regulation capacity; additionally, it serves to optimize operation of solar thermal power plants. Even though forecasting can be beneficial, accurate forecasting of ramps in solar radiation during 0 to 30 minute time frames poses unique challenges due to the small size of cloud features that have not yet been resolved by satellite or numerical weather prediction methods. The purpose of this project was to: 1. develop new solar forecasting algorithms, and 2. conduct a scaled demonstration at the 48 megawatt (MW) Sempra US Gas & Power utility solar power plant.

The second area of integration research involved energy storage. UCSD has been field testing distributed energy storage systems (DESS) since 2011. Integration of renewable generation through battery chemical energy storage is relatively new since energy storage systems for commercial and behind-the-meter applications have little long term performance history. One of the first community size energy storage systems in the United States, a 30 kilowatt (kW) by 30 kilowatt hour(kWh) system, was installed at the University of California, San Diego campus and was integrated with a dedicated 30 kW photovoltaic (PV) array in 2011. Deployment of energy storage is an important factor that will enable reliance on renewable energy generation as an efficient, reliable, cost effective source of energy generation in California. The purpose of this energy storage demonstration project was to: (1) provide stable and efficient energy, (2) to store solar energy and inexpensive night-time energy (from commercial grid) and use at peak time to lower the energy cost and demand charge, and (3) to provide ancillary function (like emergency power back up for communication).

UCSD's third project was working with EV charging manufacturers and automobile manufacturers to develop and test new forms of EVs powered by renewable generation. In 2012, a collaborative group was established to develop the testing and feasibility of EV renewable charging; the parties involved included UCSD, San Diego Gas & Electric (SDG&E), the City of San Diego, Cleantech San Diego, and General Electric. The demonstration project was developed at the world famous San Diego Zoo where a 90 kW photovoltaic array, five EV charging stations, and a 100 kW by 100 kWh energy storage system were installed. The project

analyzed the feasibility of solar to EV charging and the impacts of EV and PV on distribution systems.

The last project the researchers invested in was overall microgrid situational awareness. UCSD provided direct access and observational capability of the UCSD microgrid to California Independent System Operator (CAISO). This unique observability allows CAISO to better understand how microgrids operate and how they may interact and participate in CAISO energy markets in the future. With the objective of learning more about potential CAISO market participation with existing and potential microgrid capability, UCSD participated in the CAISO Fall 2013 market simulation. Within the UCSD microgrid capability, two resource types were created and modeled in the CAISO market test environment for use during the simulation. The simulation itself was conducted to test new market features that were scheduled for deployment to the production market and included a full representation of system-wide activity and resource participation.

Project Results

The efforts of the research conducted within this report resulted in the use and application of approximately 5.8 megawatts (MW) in renewable resources. The University of California, San Diego not only implemented one of the most automated microgrids to date, but also provided the most energy storage of any microgrid within the United States.

For the solar forecasting project, two methods were developed and implemented at a utility-scale solar power plant (Figure ES-1) using two different data sources: (1) ground-based visible imagery from two total sky imagers (TSIs), and (2) a spatially distributed inverter power output, located at the plant, paired with measurements of cloud speed and direction (also known as Cloud Speed Persistence).

Figure ES-1: 48 MW Section of the Sempra US Gas & Power Copper Mountain Solar Power Plant

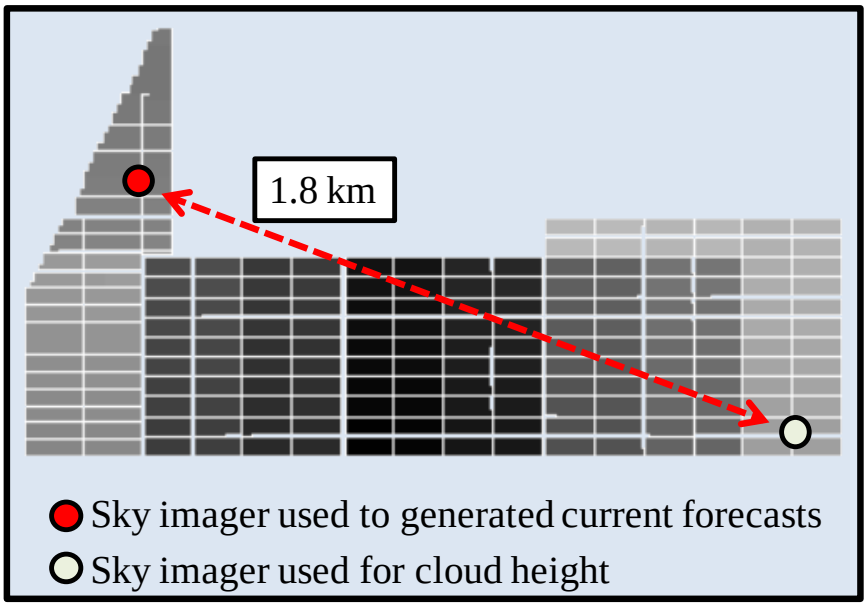

Outline of the 48 MW section of the Sempra US Gas & Power Copper Mountain Solar power plant. One forecast method uses sky imagers at the locations indicated; the other method uses inverter power output and each inverter's panel footprint is shaded with a different gray level.

The performance results for the selected week indicate that more work is required to make sky imagery based short-term forecasting a viable technique. The key finding in this study is that the total sky imager (TSI) as an instrument is not suitable for generating short-term solar power forecasts primarily due to the shadow-band and low image resolution. Image processing algorithms to reliably detect clouds near the sun and the horizon will also have to be improved. The University of California, San Diego has since addressed these issues through the development of new instrumentation and improved algorithms.

The cloud speed persistence method consists of advecting, or transporting, the current distribution of power output across the plant using measurements of cloud motion vectors, shown in Figure ES-2. Cloud motion vectors can be obtained from cloud arrival times at a triplet of inverters. The initial power output distribution is then advected across the power plant.

Figure ES-2: Illustration of the Cloud Speed Persistence Approach

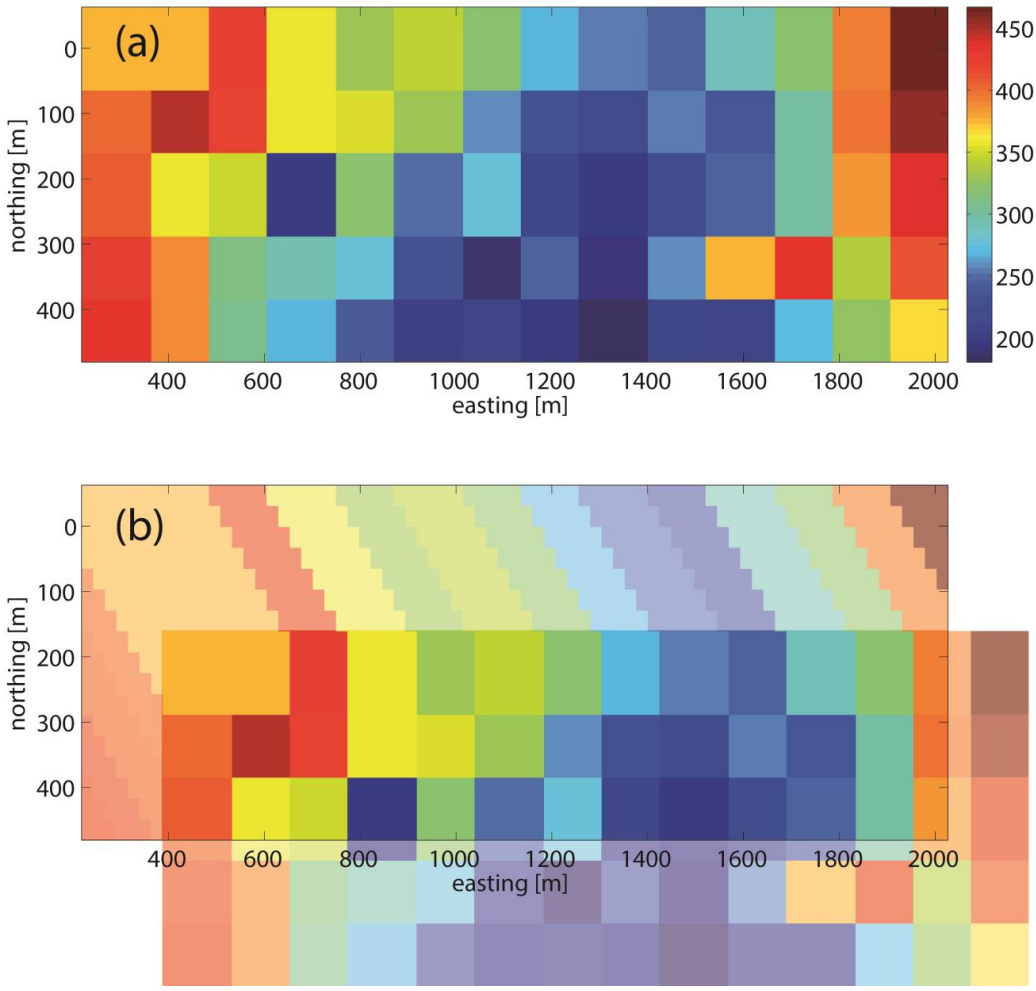

Inverter power output distribution (Kw) at the forecast issue time and (a) as forecast 8 seconds later, (b) each box represents one inverter. The direction of cloud motion is south-east-ward.

Ramp persistence is up to 45 percent more accurate than persistence for very short forecast horizons. The ramp persistence accuracy decays quickly for forecast horizons greater than 30 seconds. Cloud speed persistence is a consistently skillful forecasting technique which beats persistence over all forecast horizons and by up to 15 percent. The median forecast horizon for which the initial power output distribution was not completely advected outside of the plant footprint was 54 seconds. Cloud speed persistence forecasts using only power plant data are relatively easy to setup and can be valuable in controlling power plant ramp rates through energy storage or inverter curtailment.

As for the energy storage research, the 30 kW by 30 kWh distributed energy storage system supplied by Sanyo-Panasonic was integrated with 30 kW of roof top PV system . It consisted of compact interchangeable battery modules (like the DCB-102) with an output of 48 volts (39 to 52 volt max) and a charging current of 10 amps. Testing showed the battery charge and discharge efficiency at 97.6 percent, while the total charge and discharge system roundtrip efficiency totaled 86.8 percent, also shown in Figure ES-3).

Figure ES-3: Sanyo-Panasonic Energy Storage System Efficiency

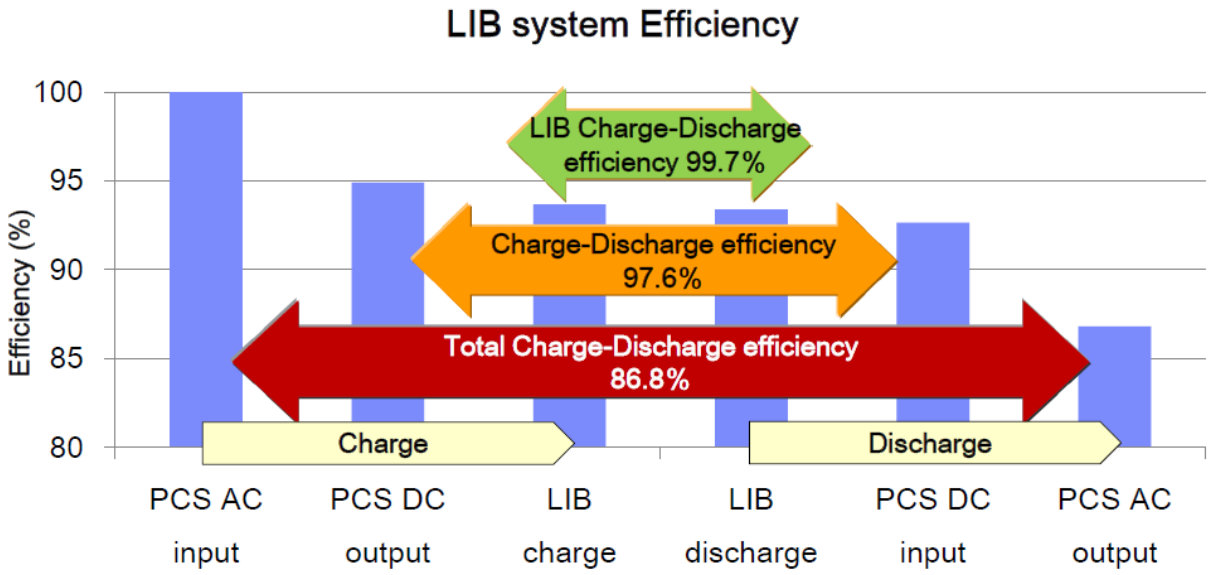

Testing showed the battery charge and discharge efficiency at 97.6 percent, while the total charge and discharge system roundtrip efficiency totaled 86.8 percent.

The second DESS consisted of 125 kW by 65 kWh of energy storage, operating on four used PEV battery packs. The control algorithms developed for the DESSs accept solar forecasting information and support DESS using the following applications:

- Smoothing of renewable intermittency
- Peak load reduction using stored solar PV generation
- Energy arbitrage
- Frequency regulation
- Demand charge management
- Regulation energy management

Results of this testing indicate that the overall DESS performance and life expectancy are highly dependent on the use regarding application of the DESS. The performance is also highly affected by the design and control of the battery management and power management systems employed for the DESS.

Two resources, one which represented a behind the meter demand response and the other a bi-directional storage resource, were bid into the CAISO market test environment over a number of weeks for a variety of products that included economic energy and frequency regulation. The bids successfully cleared the markets and returned data sets that can be used for further analysis, as well as three days of "bid to bill" data that provide insight into the full financial scope of market participation. While the prices returned from the market simulation cannot be

used to project the potential revenue for wholesale market participation, the underlying data provides a framework for further analysis utilizing production prices. Perhaps of most use is the data returned on the bi-directional storage resource participating in frequency regulation, which provides insight into how storage capability with the primary purpose of supporting photovoltaic (PV) would be dispatched by the CAISO.

Project Benefits

The project researched variety of technologies to facilitate solar power integration; due to their promising results, these technologies are now becoming more widely adapted. The sky imager technology was the first to be deployed at a utility scale solar power plant.Energy storage and microgrid situational awareness have become very active areas and the lessons learned through the UC San Diego deployments continue to reverberate through the industry and policy. The concluded research will help California establish renewable energy integration into the electrical grid while also providing more stable, renewable sources of energy for the state.

CHAPTER 1: Introduction

The impact of high levels of PV penetration on the distribution system has become a concern to utility operations and customer power quality. One of the major concerns is the potential impact of the rapid fluctuations of distribution voltages and line loading caused by the intermittency of PV due to the passing of clouds. A variety of mitigation measures exist, including solar forecasting, energy storage, and EV charging. Coordination of these measures within a microgrid and coordination between the microgrid and the system operator provide the most efficient utilization of resources and increase the permissible limits of high PV penetration.

The UCSD and California ISO are working together to investigate how microgrids could integrate with the electric power grid and participate in the ISO wholesale electricity markets as flexible energy resources. Flexible energy resources are resources that can respond in ways that help mitigate many of the operational challenges that we expect to see as a result of greater amounts of intermittent and variable renewable generation connecting to the grid to meet the 2020 33% Renewables Portfolio Standard (RPS) target in California. In general, flexible resources are resources that can:

- React quickly and meet expected operating levels
- Sustain upward or downward ramps
- Start and stop multiple times per day
- Respond for a defined period of time
- Change ramp directions quickly
- Start with short notice from a zero or low-electricity operating level
- Accurately forecast operating capability

For microgrids to be effective grid resources, participation protocols and procedures need to be understood and further developed by the California ISO and microgrid developers to ensure reliable and efficient operation of microgrids within the ISO control area. Microgrids offer an alternative architecture to the conventional large scale interconnected network with central power plant dispatch. Potential benefits of microgrids include increased reliability, lower operational costs on a local basis, and more efficient use of distributed renewable generation.

Within a microgrid, the large short-term power output variability of solar photovoltaic (PV) power plants caused by changing cloud cover is a major obstacle to high solar power penetration and autonomous operation. To maintain electric balancing in a (micro)grid with variable renewable energy generation such as PV, conventional rampable power plants or energy storage systems are needed. Forecasting improves design and operation of such ancillary services, especially under conditions of large ramp rates[1,2]. For predicting solar

[1] Mammoli, A., Menicucci, A., Caudell, T., Ellis, A., Willard, S., & Simmins, J. (2013). Low-cost solar micro-forecasts for PV smoothing., (pp. 238-243).

irradiance one to several days ahead, numerical weather prediction models are advantageous since they take into account atmospheric phenomena as cloud formation, evaporation and atmospheric (see Coimbra et al.[3] for a review). Since NWP lack granularity and computational efficiency, very short-term forecasts (covering a horizon of up to 30 min) are primarily obtained by calculating the motion of clouds with sky imagers or satellite data. Still, physically-based forecasting alone often presents worse aggregate errors than naive persistence forecasts. In specific, for satellite imagery, (1) satellite cloud motion vectors are determined from synoptic cloud fields while local clouds may deviate from that velocity and (2) satellite imagery does not have the granularity to resolve within-plant differences in solar irradiance. In this report, two nowcasting methods that explicitly take advantage of the embedded cloud motion information are further developed and demonstrated.

To mitigate forecast errors or shape the load curve for more economical energy procurement, energy storage systems can act as load sinks or provide local generation. UCSD has been field testing a few distributed energy storage systems (DESS) since 2011. Battery chemical energy storage for supporting integration of renewable generation is relatively new, and DESSs for commercial and behind the meter applications have little long term performance history. One of the first community size energy storage systems, 30 kW / 30 kWh, in the US was installed at the University of California – San Diego campus and was integrated with a dedicated 30 kW photovoltaic (PV) array in 2011. Deployment of energy storage will be an important factor that will enable reliance on renewable energy generation as an efficient, reliable, cost effective source of generation in California. The purpose of the demonstration energy storage projects was:

- Test peak shaving to reduce the energy use/cost.
- Provide stable and efficient energy.
- Store solar energy & inexpensive night-time energy (from commercial grid) and use at peak time to lower the energy cost.
- Ancillary Function (emergency power back up for communication etc.)

A special case of energy storage is electric vehicles (EVs). Electric transportation using local renewable generation offers the ultimate in clean transportation, and when coupled with energy storage, offers a potentially economical source of energy for vehicle charging. SDG&E, working with UCSD and Smart Cities partners, developed and tested a solar PV system directly coupled with electric vehicle (EV) charging and energy storage. This system was installed at the San Diego Zoo and was made completely available to the public. This report provides a summary of the analysis of the data of EV charging use, solar PV power production and energy storage acting in conjunction to reduce grid impacts of high PV penetration.

The report is structured as follows. First the hardware deployed is described in Section 2. Applications of the hardware to facilitate solar power integration are presented in Section 3.

---

[2] Mills, A. D., & Wiser, R. H. (2012, 06/2012). Changes in the Economic Value of Variable Generation at High Penetration Levels: A Pilot Case Study of California.

[3] Coimbra, C. F., Kleissl, J., & Marquez, R. (2013). Chapter 8 - Overview of Solar-Forecasting Methods and a Metric for Accuracy Evaluation. In J. Kleissl (Ed.), *Solar Energy Forecasting and Resource Assessment* (pp. 171-194). Boston: Academic Press.

Section 4 summarizes lessons learned from these demonstration projects. Conclusions are presented in Section 5.

CHAPTER 2:
Hardware Deployments and Control Algorithm Development for Solar Power Integration

2.1 30 kW by 30 kWh PV Integrated Energy Storage

UCSD and Sanyo (later Panasonic) jointly developed the concept of demonstrating energy storage to make PV more dispatchable and to improve PV performance. A 30 kW by 30 kWh energy storage system with corresponding 30 kW PV array was installed at the La Jolla Playhouse and was operational by November, 2011. The system was decommissioned from service in June, 2014.

The project was interfaced with UCSD's solar forecasting system, and testing focused on firming renewables, smoothing of intermittency, and peak load shifting use cases. This system was one of the first distributed energy storage systems (DESS) integrated with PV solar and installed in California, in fact at the time this was one of the first DESS installed in the US, and thus has been in operation collecting the most data for DESS. Figure 1 shows the schematic summary of the DESS and how it is integrated with PV solar and local distribution customer load.

Figure 1: Sanyo Dess System Summary

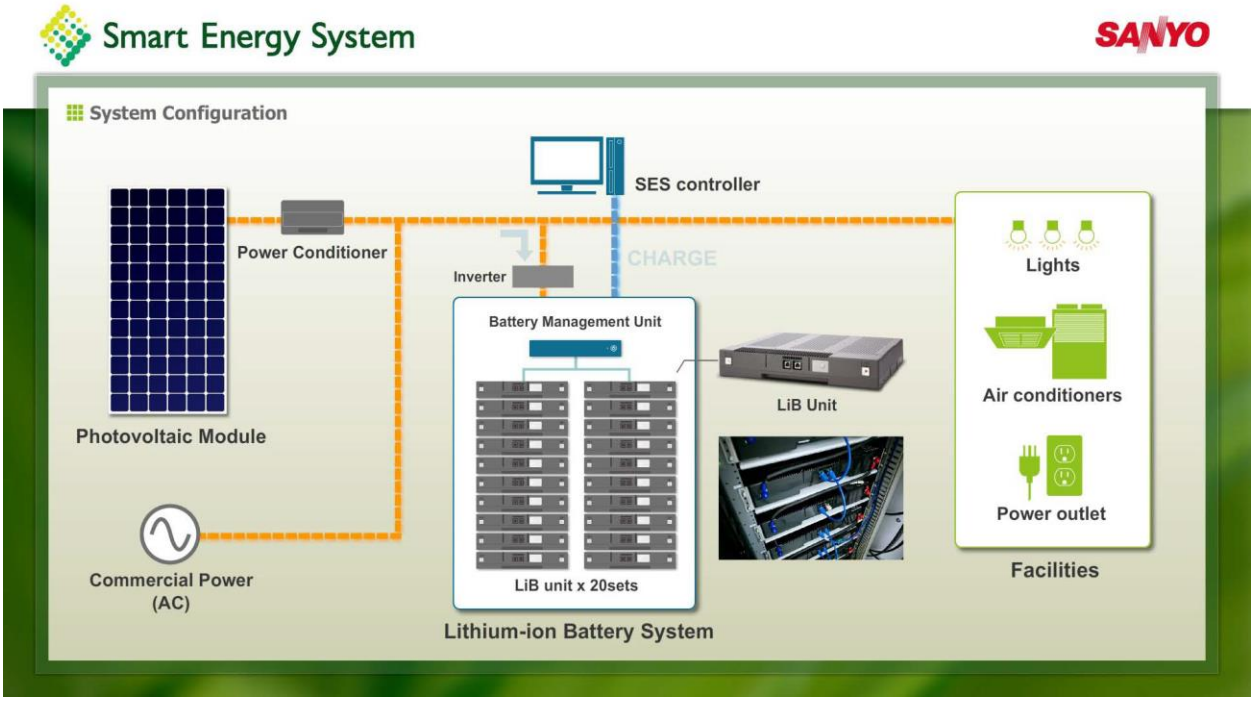

The schematic summary of the distributed energy storage systems (DESS) and how it is integrated with PV solar and local distribution customer load.

Source: Sanyo / Panasonic Corp.

The DESS utilizes lithium-ion batteries that are packaged in modules; each module contains 312 standard P18650 batteries. Each module is rated at 1.6 kWh, there are a total of 20 modules in the container (Figure 2). The DESS is connected to the same AC power system as the 30 kW PV solar system and the PV solar inverter and DESS inverter are designed to work in concert through a local control and monitoring system. The 30 kW PV solar system is located on the roof of the adjacent Mandel Weiss Theater and consists of 150 Sanyo panels.

Figure 2: Sanyo DESS Battery System and PV Solar Panels

The DESS utilizes lithium-ion batteries that are packaged in 20 modules per container.

Photo Credit: UC San Diego

The DESS controller is designed to control charge and discharge of the batteries to stabilize the power use and reduce peak demand. Also energy arbitrage has also been utilized to charge the DESS during off peak hours when energy costs are lower, and discharged later to meet theater peak load requirements.

2.2 125 kW by 65 kWh EV Battery Test Stand DESS

An energy storage system test stand was installed at UCSD utilizing 2nd life plug-in electric vehicle (PEV) batteries. This energy storage testing included partners California Center for Sustainable Energy (CCSE), National Renewable Energy Laboratory (NREL), San Diego Gas & Electric (SDG&E), AeroVironment, BMW Group, and University of California, Davis. The purpose of this testing is to study the viability of using PEV battery systems in the grid.

The Battery Test Facility was a $220,000 hardware installation located at Hopkins Parking Structure. It was commissioned in February 2012. Its flexible platform allows for easy replacement of batteries and the ability to switch out one for another. At any one time, the test bed can operate up to four full size EV battery packs (with a 120 kW peak total battery power limit) with independent control channels, and data acquisition. The Battery Control Software (BCS) was specially designed by AeroVironment to provide local and remote control of the batteries. The Battery Control Software communicates with each battery's Battery Management System (BMS) individually via CANbus to command the battery. Remote control of the Battery Control Software can be performed via Modbus.

To simulate demand charge management, a solar forecast, building load forecast, and battery dispatch are generated once per day. Each minute, the algorithm reads in real-time building load and PV generation data and makes updates to the battery dispatch. The dispatch is grabbed by Power Analytics' Paladin software and Modbus commands are sent to the Battery Control Software by Paladin. The DCM algorithm tracks the SOC of the battery virtually. To mitigate any issues of the algorithm "battery" and the real batteries' SOC's being out of sync, there is an SOC synchronization and maintenance of the batteries (cell balancing) once per day at 3:00 am. At 3:00 am, the Paladin software overrides control of the batteries and taper charges and balances them to 100%. At 5:00 am, control is handed back to the DCM algorithm which resets its SOC counter to 100%. The batteries in our test facility are around 20 kWh each and they are of different chemistries which makes this configuration a world's first.

2.3 Renewable Energy Electric Vehicle Charging at San Diego Zoo

Smart City San Diego (www.SmartCitySD.org) is a collaboration of the City of San Diego, San Diego Gas & Electric, General Electric, UC San Diego and CleanTech San Diego. Together, these leading organizations from government, business, education and non-profit are maximizing synergies to drive existing energy programs forward, identify new opportunities, and move the San Diego region beyond today's boundaries of sustainability.

One of the first of its kind in the country, the Solar-to-EV project was designed to harness energy from the sun to directly charge plug-in electric vehicles (PEVs), store solar power for future use and provide renewable energy to the electrical grid. The project incorporates 10 solar canopies producing up to 90 kilowatts (kW) of electricity – enough energy at peak capacity to power 59 homes – as well as five EV charging stations. Using new battery technology, a 100-kW/100-kWh energy storage system is charged by the solar canopies and used to offset power demand on the grid to charge the vehicles. The storage system was sized to 100 kW based on the available grid tied inverter size also it closely matches the PV power rating (90 kW), thus the inverter for the battery system can absorb and capture all of the PV power when it is generating at full power. When the battery is full and solar production exceeds EV charging demand, the excess solar energy that is generated is put onto the electric grid to improve reliability and benefit the surrounding community. The solar canopies also provide shade to approximately 50 cars in the Zoo's southeast parking area (Figure 3).

Figure 3: Smart City Renewable Energy Charging Project

Ten solar canopies rated at 90 kW installed at the San Diego Zoo's parking lot.

Photo Credit: San Diego Gas & Electric Co.

The equipment used consists of the following:

(1) Princeton Power Systems DRI-100 Inverter: Rated at 100 kW @ 480V AC. Two (2) DC Ports (Solar+Battery) rated at 100 kW DC each.

(2) Kokam KBR100 Lithium-Ion Battery System with BMS: Rated at 100 kW/100 kWh.

(3) (420) Kyocera KD245GX Modules: Rated at 245W STC/219.1W PTC

(4) (4) Blink Level 2 Wall Mount Chargers: Rated at 7 kW (max)

(5) Blink Level 2 Pedestal Charger: Rated at 7 kW (max)

The Princeton Power DRI-1000 inverter converts DC power to AC Power and feeds it to the grid. It has two DC input ports, one of which is connected directly to the DC output of the PV panels,

and the second one is connected to the Kokam Lithium-ion battery system. This topology allows centralized control and conversion, allowing PV power to be routed directly to the energy storage or to the grid thus minimizing conversion losses and optimizing the dispatch of energy to the grid or for end use.

The City of San Diego worked with representatives of the San Diego Zoo to dedicate a portion of the public parking lot as the venue for this project. It has enabled the stakeholders to gain real world experience with renewable EV charging and to demonstrate and promote clean transportation. Construction began on September 4, 2012 and was completed in November, 2012. Commissioning of the entire system was completed and the system was energized on April 26, 2013.

2.4 Solar Forecasting at a Utility Scale Power Plant

Intra-hour solar forecasting can support ramp rate control and 5 minute dispatch by a system operator. Sky imagers are uniquely suited for these short time horizons of up to 20 minutes ahead. However, cloud detection in the solar region of the image is challenging. Therefore, simple persistence models or more advanced machine learning techniques are often used for nowcasting. However, information about the cloud speed, which is critical to describing the translation of sky conditions across the power plant is typically not used explicitly in these models. While cloud speed sensors are not yet standard, Bosch & Kleissl[4] showed that cloud motion can also be detected from spatio-temporal irradiance or power measurements across the PV plant. Cloud motion vectors (cloud speed and cloud angle) were determined from the timing of cloud arrival at three different points. This method was applied in this project to generate forecasts at a utility scale solar power plant, as an alternative to sky imager forecasts.

2.4.1 Sky Imagery and Inverter Power Output Data

Solar power output data of 96 500kW inverters from the Sempra US Gas and Power 48 MWAC Copper Mountain Solar 1 PV Plant at Henderson, NV, was acquired with a sampling rate of 1 s. Fifteen calibrated reference cells provided plane-of-array global irradiance (GI) at 1 sec and five weather stations provided standard meteorological measurements including plane-of-array GI and GHI from Kipp & Zonen CMP11 broadband pyranometers. The PV plant (35.78° North; 115.00° West) covers a surface of 1.89 km2 with thin-film Cd-Te panels[5] and generation is fed into the CAISO grid. For the ramp forecasting approach, for generality, only a rectangular part of the plant with 70 inverters is considered, spreading 1807 m in the east-west and 539 m in the north-south direction (Figure 4).

Two Total Sky Imagers (Yankee Environmental Systems Inc., TSIs) were also installed at the plant to validate the sky imager forecast methodology in a utility-scale environment. The TSIs were spaced 1.8 km apart using the configuration shown in Figure 4. The sky imagers were installed on June 17, 2011 and high quality imagery has been acquired near continuously since August 5th, 2011. The imagery is streamed in real-time to the CAISO renewables desk.

---

[4] Bosch, J. L., & Kleissl, J. (2013). Cloud motion vectors from a network of ground sensors in a solar power plant. *Solar Energy , 95*, 13-20.

[5] First Solar. (2011). Copper Mountain Solar 1 Datasheet. *Available through: http://www.firstsolar.com/Projects/Copper-Mountain-Solar-1 (Accessed 23 May 2013)*

Figure 4: 48MW Section of the Sempra US Gas and Power Copper Mountain Solar Power Plant

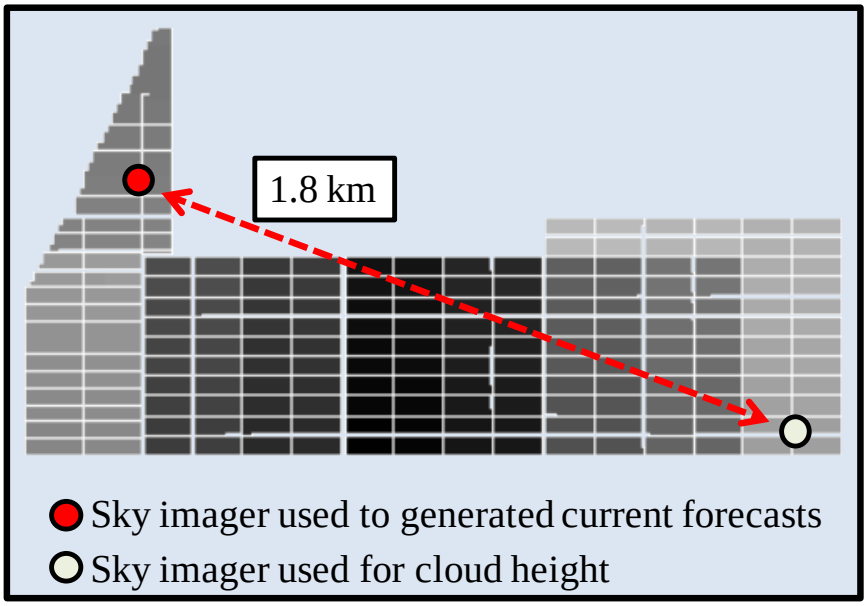

Outline of the 48MW section of the Sempra US Gas and Power Copper Mountain Solar power plant, with sky imager locations indicated. Each inverter's panel footprint is shaded with a different gray level.

Figure 5: Satellite Photograph of the Sempra US Gas and Power CMS1 Photovoltaic Plant

Satellite photograph of the Sempra US Gas and Power CMS1 photovoltaic plant near Henderson, NV[6]. Only the 70 inverters within the black box were considered for the analysis.

Photo Credit: Google Earth.

2.4.2 Cloud Speed Persistence Forecast Method

Cloud velocity vectors are derived as in Bosch & Kleissl[7] using triplets of inverters to measure the time delay between the arrival of the cloud at different sensors. Average cloud speeds are 21.6 m s^{-1}. About 12 months of data are available (Jul 6 2011 to Jul 11 2012), but after discarding completely clear days only 171 days remained for further analysis.

Standard and ramp persistence methods are used as benchmarks to evaluate the new cloud speed persistence forecasting method. Generally, persistence is based on the assumption of no change in sky condition or constant clear sky index, see Eq. 1; changes in power output due to the change in solar position are accounted for by the use of the Ineichen clear sky model, modified by Perez et al. and extended to tilted surfaces as in Page. The clear sky model is used to calculate the change of the plane of array irradiance (POA_{CS}) over the forecast horizon. Assuming a constant PV efficiency throughout the forecast horizon, forecast power output is adjusted by the relative change in POA_{CS}.

$$\text{Equation 1: } P_{Persistence}(t) = \min \left[P(t = 0s) \cdot \frac{POA_{CS}(t)}{POA_{CS}(t=0)}, 35\ MW_{AC} \right]$$

[6] Google Earth. (2013). PV Plant at Henderson (NV) 35°47'00.06"N, 114°59'33.10"W, elevation 564 m.

[7] Bosch, J. L., & Kleissl, J. (2013). Cloud motion vectors from a network of ground sensors in a solar power plant. *Solar Energy , 95*, 13-20.

Ramp persistence projects the *change* in power output over the last second to persist for the forecast period, see Eq. 2.

Equation 2: $$P_{Ramp}(t) = \min \ [P(t = 0s) - P(t = -1s) + P(t - 1s), 35\ MW_{AC}]$$

The minimum and maximum power outputs are constrained between zero and the AC rating of the inverters (35 MW_{AC}), respectively. Clear sky corrections are not applied for ramp persistence since clear sky irradiance changes are approximately linear over these short forecast horizons.

Cloud speed persistence: Cloud motion is used in combination with the spatial distribution in solar power output at the forecast issue time to forecast power output of the plant. Conceptually, the initial power output map (e.g. Figure 6a) is moved along the vector of cloud motion.

Figure 6: Inverter Power Output Distribution

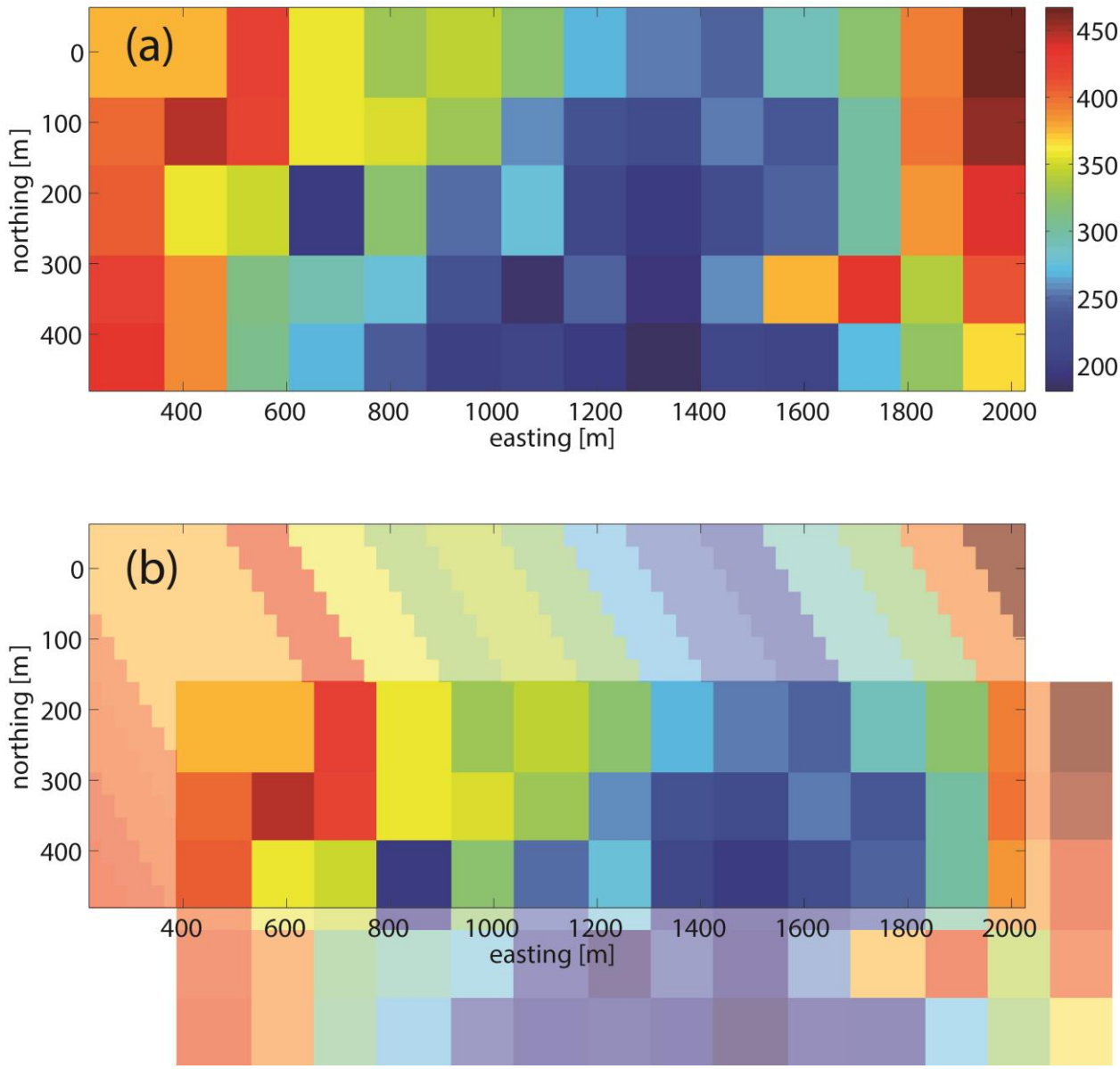

Inverter power output distribution [kW] at a) t=0 s as measured at 1335 PST on Jan 4 2012 and at b) t=8 s as forecast with cloud speed persistence. The origin of the coordinate system is at the North-West inverter.[8]

[8] Lipperheide, M., JL Bosch, **J Kleissl**, Embedded nowcasting method using cloud speed persistence for a photovoltaic power plant, *Solar Energy*, doi:10.1016/j.solener.2014.11.013, 112: 232–238, 2015.

The distance in x- and y-direction at which the initial power output map is shifted for one timestep of the forecast (Δt = 1 s) is determined from the cloud speeds (v_x and v_y) in both spatial directions

$$\text{Equation 3:} \qquad \begin{pmatrix} \Delta x \\ \Delta y \end{pmatrix} = \begin{pmatrix} v_x \\ v_y \end{pmatrix} \cdot \Delta t.$$

Some parts of the map will be shifted outside the boundaries of the power plant and will not be considered in the forecast. For the same reason other parts of the power plant in the opposite direction will not be covered by the shifted map and persistence is assumed instead (**Figure 6b**). The forecast horizon for which the cloud speed persistence forecast applies directly is therefore determined by the geometrical dimensions of the power plant and the cloud motion vector as min(L_y / v_y; L_x / v_x). The larger the cloud speed and the smaller the plant dimensions, the faster the initial power output map is advected over the power plant and leaves the boundary of the plant. When that occurs the forecast horizon of the cloud speed persistence method (see Fig. 5 later) is extended through a "delayed" persistence model assuming the forecast power at min(L_y / v_y; L_x / v_x) to persist.

Forecast results are compared using the relative root mean squared error (rRMSE) of the mean power output of the 70 inverters

$$\text{Equation 4:} \qquad rRMSE = \sqrt{\frac{1}{n}\sum_{i=1}^{n}\left(P_{forecast}(t) - P_{real}(t)\right)^2}\,\frac{1}{\overline{P_{real}}},$$

where n is equal to the forecast data points in an analyzed time interval and an overbar denotes time averaging during this period. The forecast skill relative to the persistence method[9] is defined as

$$\text{Equation 5:} \qquad skill = \begin{cases} 1 - \frac{rRMSE}{rRMSE_{persistence}} \; for\; rRMSE \;\leq rRMSE_{persistence} \\ \frac{rRMSE_{persistence}}{rRMSE} - 1 \; for\; rRMSE > rRMSE_{persistence} \end{cases}.$$

2.4.3 Sky Imager Forecast Method

The method used to generate sky imager forecasts for the Copper Mountain case study follows that of Chow et al.[10]. The forecast procedure is outlined in the flow chart in Figure 7. The

[9] Chu, Y., Pedro, H. T., & Coimbra, C. F. (2013). Hybrid intra-hour DNI forecasts with sky image processing enhanced by stochastic learning. *Solar Energy , 98*, 592-603.

[10] Chow, C., Urquhart, B., Dominguez, A., Kleissl, J., Shields, J., & Washom, B. (2011). Intra-Hour Forecasting with a Total Sky Imager at the UC San Diego Solar Energy Testbed. *Solar Energy , 85*, 2881--2893.

procedure is broken up into two steps - one that relies on sky imager data and one that is designed for the power plant being studied. A brief explanation of the procedure is contained within this section.

Figure 7: Flow Chart for Constructing Power Forecast in Copper Mountain Case Study

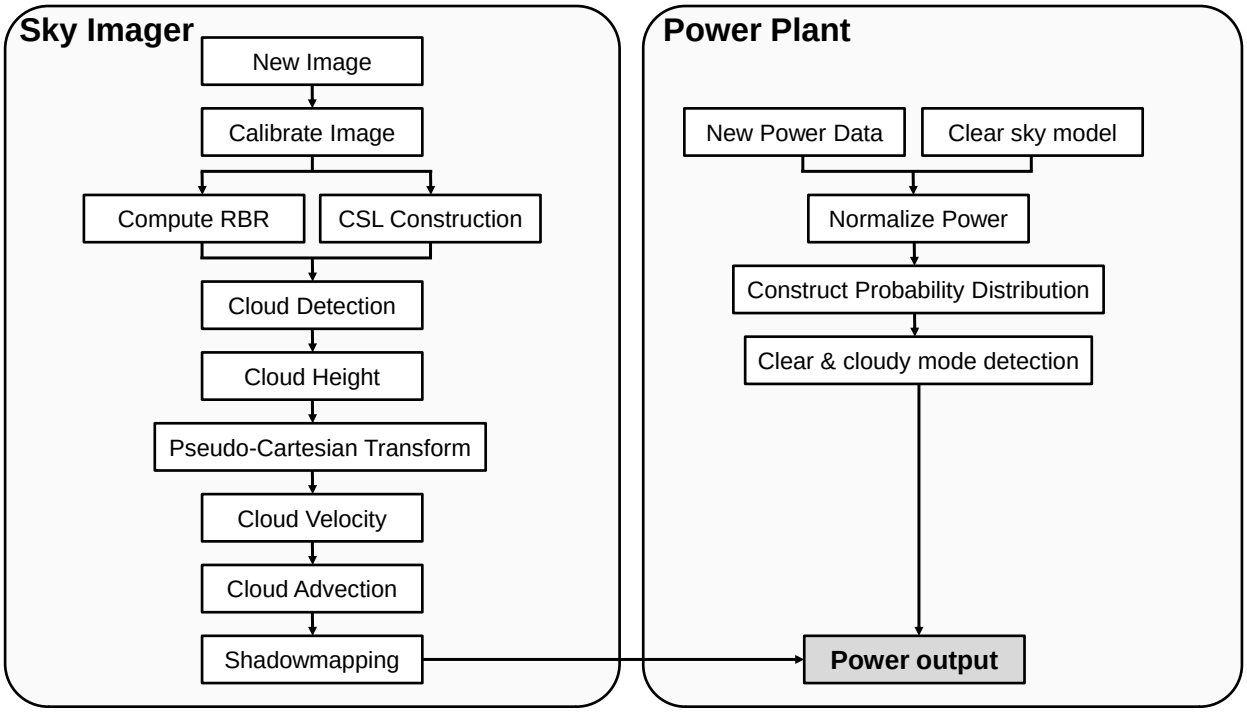

Flow chart showing the basic operations for constructing the power forecast in the Copper Mountain case study.

After a new image is collected, image specific masks (for the sun, shadowband, etc.), and a calibration map of scattering angle based on the current solar zenith angle are constructed for the entire image. Following this, clouds are detected and cloud altitude is computed. The binary cloud/no cloud information is still in the original image coordinates, but what is needed is a georeferenced mapping of the clouds. To obtain this, the pseudo-cartesian transform is applied[11], but instead of the arbitrary scaling used there, a scaling that maps cloud information to a latitude-longitude grid at the cloud altitude[12] is used. This transform requires imaging system calibration such that each pixel has a known look angle (zenith and azimuth coordinate

[11] Allmen M, and Kegelmeyer W (1997). The computation of Cloud-Base Height from paired whole sky imaging cameras. Journal of Atmospheric and Oceanic Technology ,Volume 13, 97-113.

[12] Chow, C., Urquhart, B., Dominguez, A., Kleissl, J., Shields, J., & Washom, B. (2011). Intra-Hour Forecasting with a Total Sky Imager at the UC San Diego Solar Energy Testbed. *Solar Energy , 85*, 2881--2893.

pair), i.e. the spherical coordinates without the radial dimension. The resulting georeferenced map of clouds is termed the 'cloudmap', which is a planar mapping of cloud position at a specified altitude above the forecast site. Of the two TSIs installed at the plant, only the northwestern unit was used in this case study to generate cloudmaps for forecasting. The second unit provided the cloud height only.

The cloud velocity is then used to advect the planar cloudmap to generate a cloud position forecast for each forecast interval. The cloud position every 30s is computed out to a 15 min forecast horizon for every new image captured. The forecast domain is defined by a grid overlaying the plant that is 4×4 km in size with a resolution of 2.5 m per forecast cell (1600×1600 cells), and each cell is resolved to a latitude, longitude, and altitude (the latter is obtained from a digital elevation model). For each forecast cell, a ray is traced along the vector to the sun and the intersection with the cloudmap is determined (Figure 8). If the intersected point is clear, that ground location is deemed clear, whereas if the intersection is cloudy, the ground point is deemed shaded by cloud. Repeating the shadow mapping process for each forecast cell constructs a map of cloud shadows (shadowmap). This shadowmap provides the percentage of the plant that is shaded. Shadowmaps are constructed for each advected cloudmap out to the 15 min forecast horizon (generating 30 forecasted shadowmaps).

Figure 8: How Shadowmaps are Generated From Ray Tracing

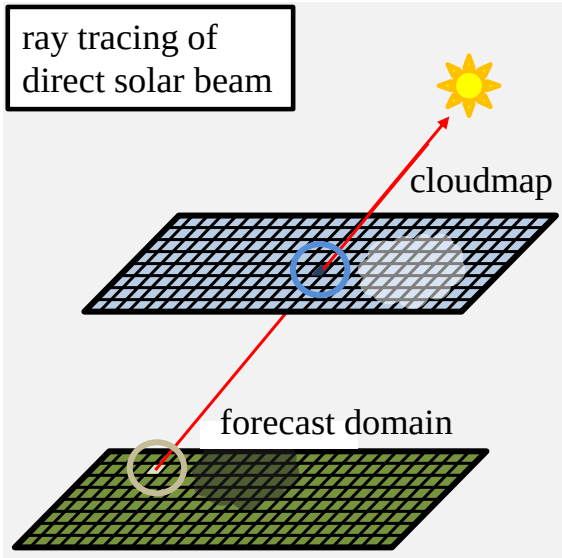

Cartoon illustration of how shadowmaps are generated from ray tracing. The dark green forecast domain is shown to be flat, but topography effects are included in actual modeling. The cloudmap is assumed flat. An example intersection is shown for a single grid cell in the forecast domain.

2.5 Microgrid Observability Test with the CAISO

2.5.1 Microgrid Connection to CAISO

As part of this project UCSD provided the CAISO access to its OSIsoft PI System to monitor microgrid operations. Integrated into the OSI PI system is the Power Analytics Paladin system

which provides analytics for the microgrid such as dynamically recalculating critical power and energy information based on the changing conditions of the microgrid. The combination of capabilities of the OSI PI server and Power Analytics provide detailed information with the purpose to enable CAISO to achieve a Deep Situational Awareness of the performance of UCSD's distributed energy resources. For example, the UCSD PI System is configurable to provide near real-time notifications to CAISO upon observed or calculated events from the UCSD Microgrid. All of these observations, calculations, and notifications are at any metered granularity of distributed energy resources including energy storage that are not typically observable since they are "behind" the utility meter. These services may be particularly important during demand responses called by CAISO and Critical Peak Pricing called by San Diego Gas & Electric (SDG&E).

Through a Remote Terminal Server, and in compliance with CAISO's and UCSD security requirements, CAISO has direct access to the UCSD PI System. CAISO is able to utilize PI Client Software and Analytics tools to visualize and analyze both real-time and historical time-series data and context from the UCSD PI system. To date the UCSD PI System acquires and stores the following data streams from the UCSD Microgrid: 107,860 regular tags at 1 sec resolution, 1096 tags associated with Phasor Measurement Units at 60 Hz, and 661 tags associated with the East Campus Substation Server. The Power Analytics model writes 17,326 tags back to the PI server.

The OSI PI environment combined with the analytics and visualization of Power Analytics Paladin system convey status and performance at a glance and provide CAISO and any authorized user the ability to view what is relevant and appropriate. Figure 9 and following show the user screens that are developed by Power Analytics Paladin control system that are available to the CAISO.

Figure 9: User Screens Developed by Power Analytics Paladin Control System

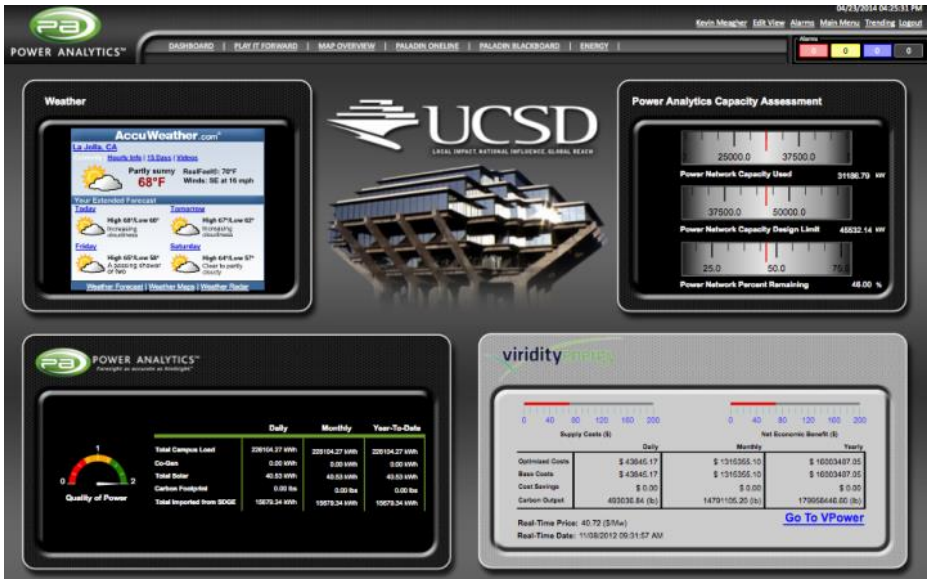

Main dashboard. Default login and overview of the UCSD Campus.

Source: UC San Diego

Figure 10: Campus Power Network

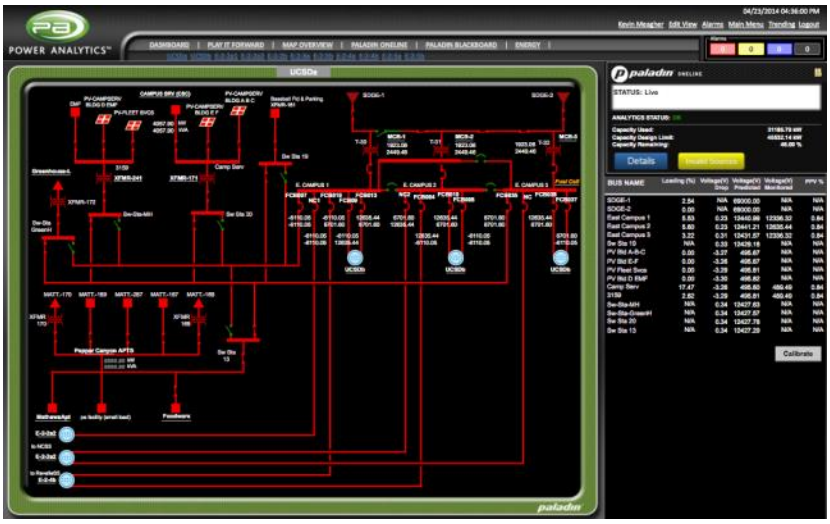

Electrical oneline of the campus animated to show status of the network with critical meter values. Predicted values are compared to actual values at key locations.

Source: UC San Diego

Figure 11: Second Life Battery Dashboard and Real Time Phasor Diagram

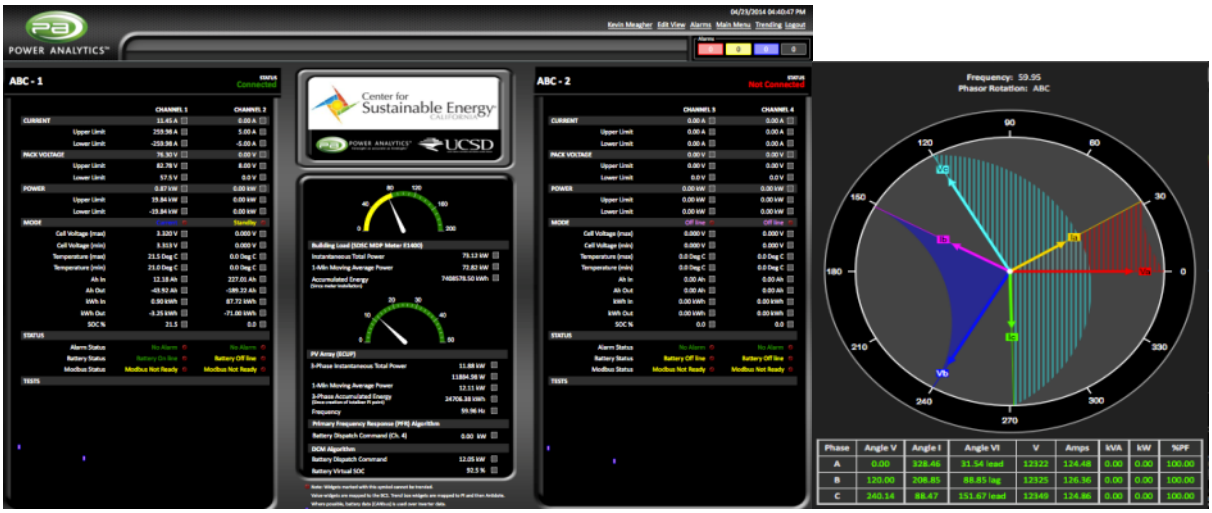

Left: Second life battery dashboard integrating used EV energy storage with photovoltaic performance. Right: Real time phasor diagram of the fuel cell power output.

Source: UC San Diego

2.5.2 CAISO Market Simulation of the UCSD Microgrid

The CAISO and UCSD have discussed how microgrids might integrate with the CAISO larger grid system, and the planning and interconnection requirements that may be needed for microgrids to interconnect and operate reliably and efficiently. The electrical grid can be broken into two levels based on its architecture and voltage. These two levels consist of the transmission system and the distribution system. The transmission system transfers the bulk of electrical energy at high voltages from generating power plants to electrical substations. Energy is then distributed to end use customers on the distribution system at lower voltages. The level at which the microgrid resource physically interconnects to the grid is extremely important in terms of interconnection rules and policies. Transmission level interconnection is managed by the ISO under federal jurisdiction. Distribution level interconnection is managed by the Utility Distribution Company (UDC) which is under the jurisdiction of the California Public Utilities Commission (CPUC).

If the resource is connected at distribution level voltages and wishes to participate in the ISO wholesale energy market, the resource must first satisfy the Utility Distribution Company (UDC) interconnection requirements and obtain an appropriate interconnection agreement, normally called a wholesale distribution access tariff (WDAT). As a wholesale resource, the microgrid could be managed to control generation or load based on a wholesale pricing. No longer does generation act primarily as a load modifier, but in conjunction with load management, may allow the microgrid to define a new level of generation export. Because loads of the microgrid are now a market commodity and will be managed based on price, consideration will need to be made to the load serving entity (LSE) that is responsible for procuring sufficient load in the service area within which the microgrid resides. Over or under procurement of load by the LSE will have financial ramifications that will need to be resolved between the LSE, microgrid resource owner, and perhaps other entities. As part of the

effort to understand how microgrids with high PV penetration would operate in within a RTO/ISO, UCSD completed a market simulation exercise with the CAISO.

Specifically, energy storage can be optimized as a wholesale market resource depending on the resource models and products offered. The intent of this effort is to participate in CAISO market simulations to explore market integration opportunities. UCSD's stated objectives were to:

- Observe various market participation options for Microgrid capabilities with both Proxy Demand Resource (PDR) and Non Generator Resource (NGR) including both NGR options, Regulation Energy Management (REM) and Non-REM.
- Obtain a "clean" Automatic Generation Control (AGC) data set for NGR operating in REM option for Frequency Regulation participation.
- Obtain "Bid to Bill" data for various products on both resource types.

To fulfill these objectives, UCSD participated in CAISO market simulations, which CAISO operates on a periodic basis to test the deployment of new market features. The market simulation of the UCSD microgrid was conducted during the September and October 2013.

CHAPTER 3:
Distributed Energy Resource Applications

3.1 Demand Charge Reduction Using Energy Storage and Forecasting

A control algorithm was developed to accept solar forecasting information and command the 30 kW / 30 kWh Sanyo energy storage system (Section 2.1) to store PV solar generated when it is generated during off peak hours, and discharge energy during on peak hours to reduce the local load and peak demand requirements. The algorithm is able to smooth out the intermittency and improves distribution system performance. This control concept was tested using the Sanyo DESS and adjacent rooftop PV. Figure 12 shows an example of how this type of control worked.

Figure 12: Example of Control Optimization System

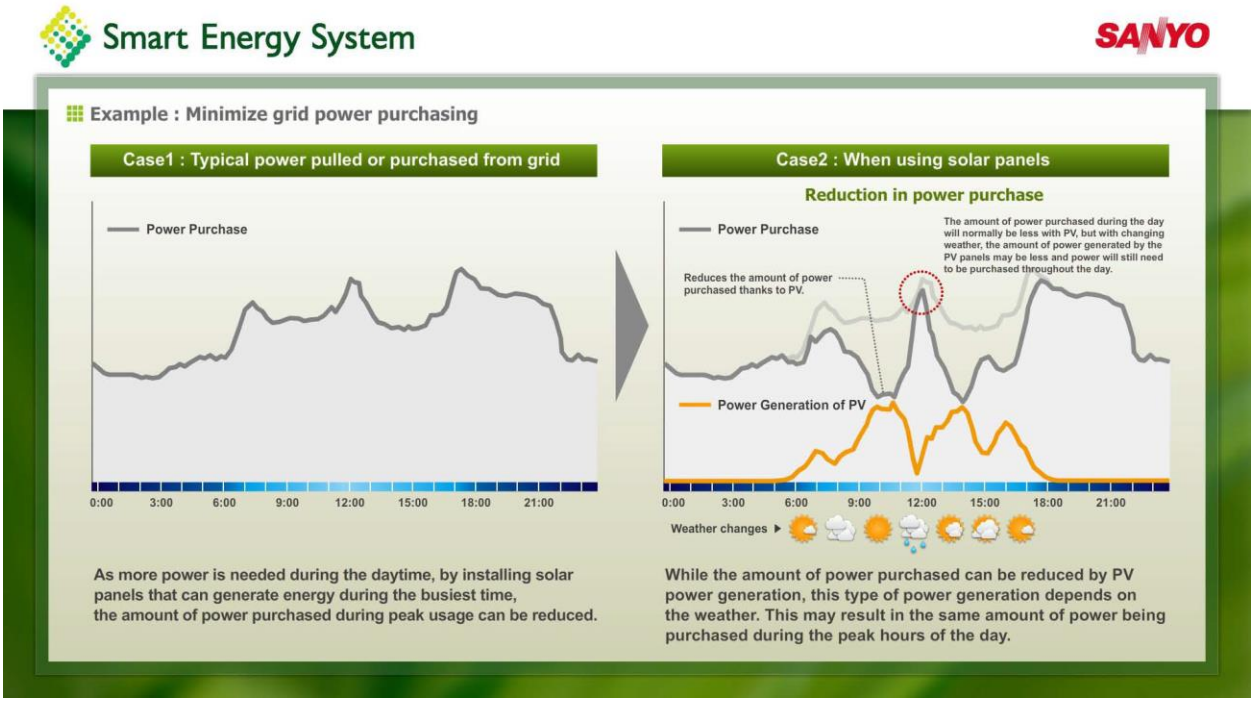

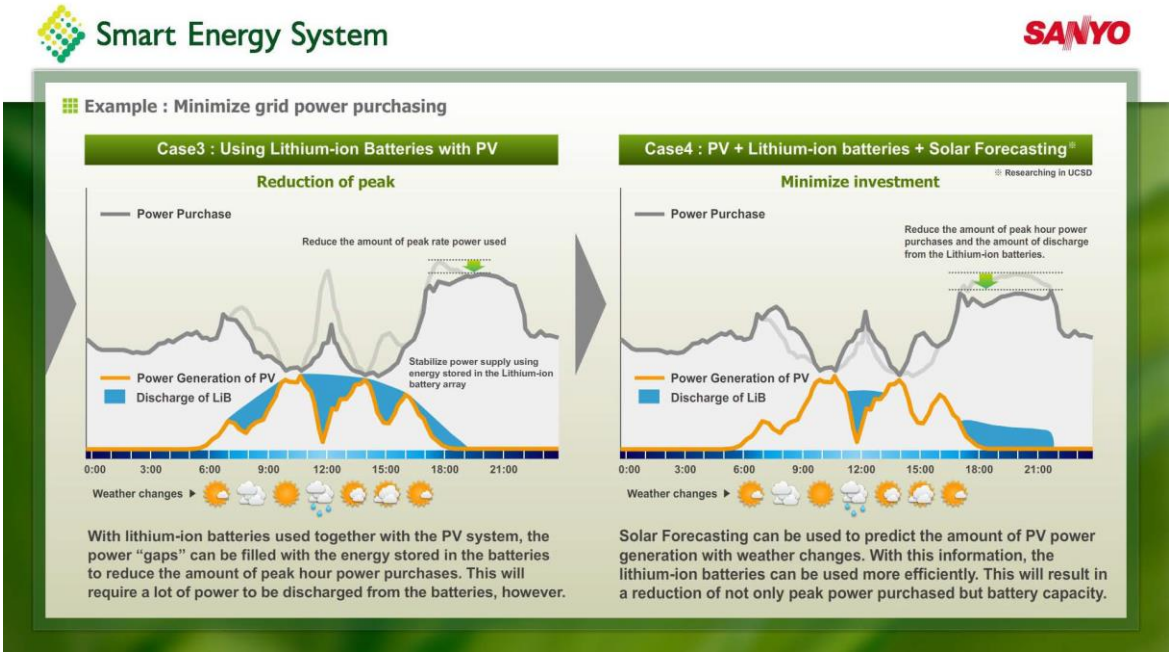

Control optimization to minimize energy costs using DESS for (Case 2) Solar PV only, (Case 3) Solar PV and energy storage, and (Case 4) Integration of PV and energy storage with solar forecasting.

Source: Sanyo / Panasonic Corp.

3.2 Battery Characterization and Use Cases for Regulation and Demand Charge Management

The first year and a half of testing of the second life EV batteries (Section 2.2) included running week-long predetermined duty cycles on the batteries. Three second-life applications were chosen for cycling because of their feasibility and economic potential. These included back-up power supply, demand charge management, and regulation energy management.

3.2.1 Battery Health Testing and Backup Power Application

The Reference Performance Test includes two parts: capacity measurements and a DC impedance measurement. The capacity measurement portion is broken up into two tests, a C/5 capacity test, and a 1C capacity test. DC impedance is measured through the pulse characterization test. The Reference Performance Test is important because it helps us to study the batteries state of health pre-second life use, and to consistently track the battery's performance and degradation under second-life use. Figure 13 shows sample data from an October 2013 C/5 Capacity Test performed on one of the batteries.

Figure 13: C/5 Capacity Test Results

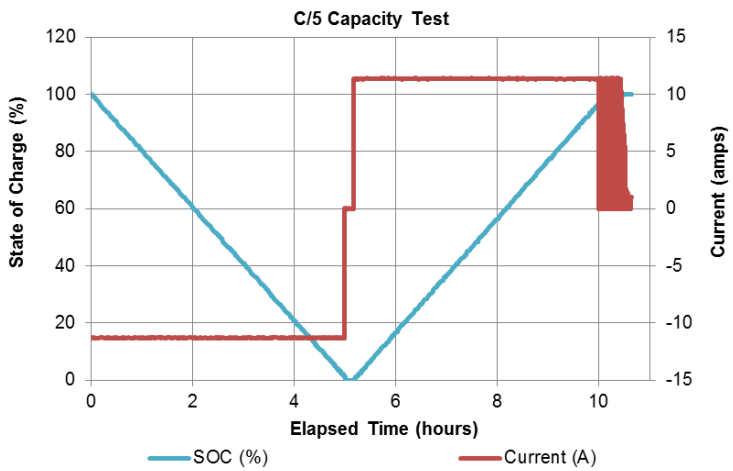

Sample data from an October 2013 C/5 Capacity Test performed on one of the batteries.

Source: California Center for Sustainable Energy

The C/5 capacity test also acts as a proxy for studying our batteries performance under the back-up power application. Because the capacity test calls for a full discharge of the battery from a fully charged state, this cycle mimics what a battery would have to do if it was needed for a back-up power application.

A pulse characterization test was also performed to measure the battery's resiliency and rise time capability. As an example, Figure 14 shows the result of running a Pulse Characterization Test on the A123 Pack #2 (Channel 3) on October 7, 2013. Pulses were 10 seconds in length at a 2.5C rate. A charge and discharge pulse was performed at 10% SOC incremented levels, with a single charge at 0% and a single discharge at 100% SOC.

Figure 14: Pulse Characterization Test

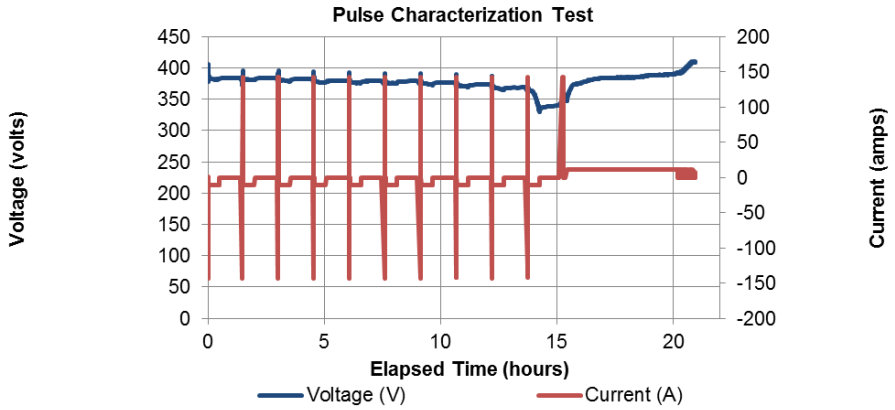

Result of a Pulse Characterization Test on the A123 Pack #2 (Channel 3) on October 7, 2013.

Source: California Center for Sustainable Energy

3.2.2 Use Case Regulation Energy Management (REM)

The duty cycle for REM was developed through collaboration between CCSE, the California Independent System Operator (CAISO) and KnGrid to study the viability of battery storage systems participating in the area regulation market. To study the viability of batteries in the regulation market, CAISO created a cycling model that mimics how generating entities respond to AGC signals which could be tested on batteries. CAISO collected AGC signals from July 1, 2010 to July, 7 2010. The economic viability was studied using these AGC signals combined with 5-minute real-time market (RTM) energy pricing data. The cycling model created from AGC signals was scaled to fit the capacity of a variety of batteries. The profile developed is what we now call a Regulation Energy Management (REM) duty cycle. Figure 15 shows the intended power profile and state of charge performance of a battery pack under REM cycling.

Figure 15: Regulation Energy Management (REM) Duty Cycle

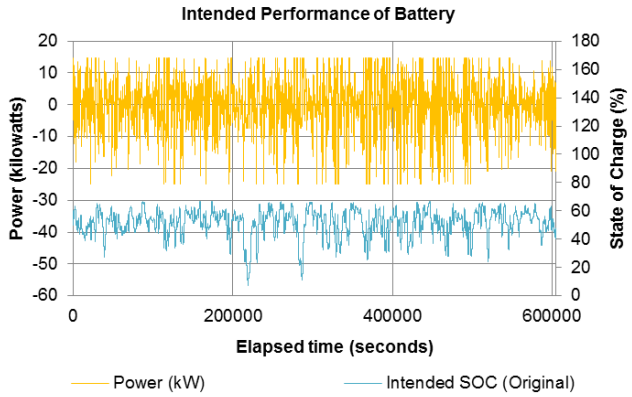

Intended power profile and state of charge of second life EV battery pack under regulation energy management (REM) duty cycle.

Source: California Center for Sustainable Energy

3.2.3 Use Case Demand Charge Management (DCM).

The DCM duty cycle was developed by NREL and UCSD based on historical building load, historical PV generation, and solar and building forecasting. **Figure 16** shows the intended power profile and state of charge performance of a battery pack under a short-term DCM duty cycle.

Figure 16. Demand Charge Management (DCM) Duty Cycle

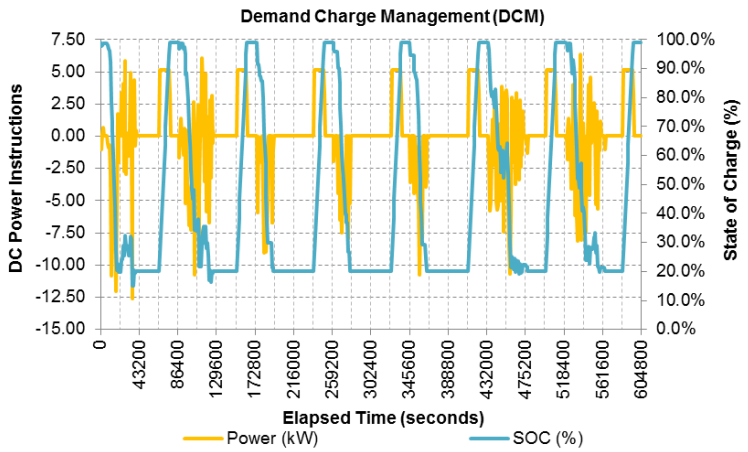

Intended power profile and state of charge of a second life EV battery pack under demand charge management (DCM) duty cycle.

Source: California Center for Sustainable Energy

3.3 Peak Shifting and Solar Variability Smoothing with Energy Storage

Use cases for the renewable EV charging project at the San Diego Zoo were PV smoothing and peak shaving, where limits were imposed on how the amount of energy stored is dispatched to the grid. Because the PV generation is entirely dependent upon solar and weather conditions, and the EV charging power consumption is dependent on when EV customers decide to charge up their vehicles.

The 100 kWh energy storage system provides great flexibility in meeting load requirements. For this project, energy storage provides the ability to store PV generation and to selectively use it for EV charging, to extend renewable energy availability after sunset, and to reduce the load impact on the grid during peak hours. Because energy storage can be dispatched to provide support to the grid independent of PV production, it provides benefits to both the utility and the utility customers. Strategically optimizing the state of charge to accommodate predicted weather impacts, energy storage systems can smooth intermittency impacts of PV on cloudy days, extend the effective hours and utilization of renewable energy and enable multiple applications to be served simultaneously. UCSD analyzed 22 days of data in total (April 12 – April 29 and May 4- May 7, 2014). May 5 is shown in Figure 17to illustrate the performance of the control algorithm.

Peak Shifting: The intention of the energy storage scheduling was to demonstrate the ability to charge the battery during the early morning (0100-0300 h) when local distribution lines are

lightly loaded and thus minimize impact to the local distribution system, and also take advantage of the period when wholesale energy costs are at minimum. The energy storage is commanded to charge up to about 70 kW (maximum power rating of the energy storage inverter is 100 kW) at about 2 am. The Battery State of Charge (SOC) rises to about 90% and is discharged beginning at 5 pm to a minimum of about 10% (SOC) is reached, occurring over a duration of about one hour and ramped down to zero power at 6 pm. During the daytime hours between 8 am to 6 pm, the PV production is exhibited by the parabolic curve in red peaking at about 12 noon when the sun is at maximum solar irradiance.

PV Smoothing Using Energy Storage: The rapid fluctuations in PV power production exhibited by the jagged green line are caused by passing clouds. The impact of this PV intermittency has been a primary concern by utilities experiencing high penetration of PV. Since inverters do not currently are not permitted to control power, or absorb power, whatever happens to the PV production due to environmental conditions directly impacts the local power grid. For example, when a PV panel is getting direct sunlight and is producing maximum power a one per unit power factor is maintained and output voltage is maximum, then when a cloud passes over and reduces power production to 30% of maximum power the PV no longer provides voltage support and no power factor correction is provided. Depending on the location and capacity of the PV, local generation, and customer loads it is possible that this can cause localized swings in voltage, and can occur very rapidly over a few seconds.

Because energy storage can be configured to perform as a bi-directional power supply, it can rapidly respond to local voltage fluctuations and serve to both absorb power (during charging) and generate power (during discharge) it can smooth PV solar generation. Since PV solar variability is characterized by short-lived power and voltage fluctuations, it does not require much energy storage capacity (kWh) to smooth out the impacts. Therefore, control systems can make these distributed energy resources (DER) work in harmony with grid operations to provide both intermittency and peak load reduction. To achieve this control, it is critical that the energy storage SOC be continuously known, and that a target SOC be configured so that the device can be completely charged or discharged to provide enough “headroom” to allow up and down power swings of sufficient magnitude to reduce intermittency. One such control algorithm was developed and implemented for the 100 kW/kWh energy storage system at the San Diego Zoo. Figure 17 shows the ability of the energy storage system to respond to the intermittency and smooth out the impacts.

Figure 17: PV Intermittency Smoothing Using Energy Storage

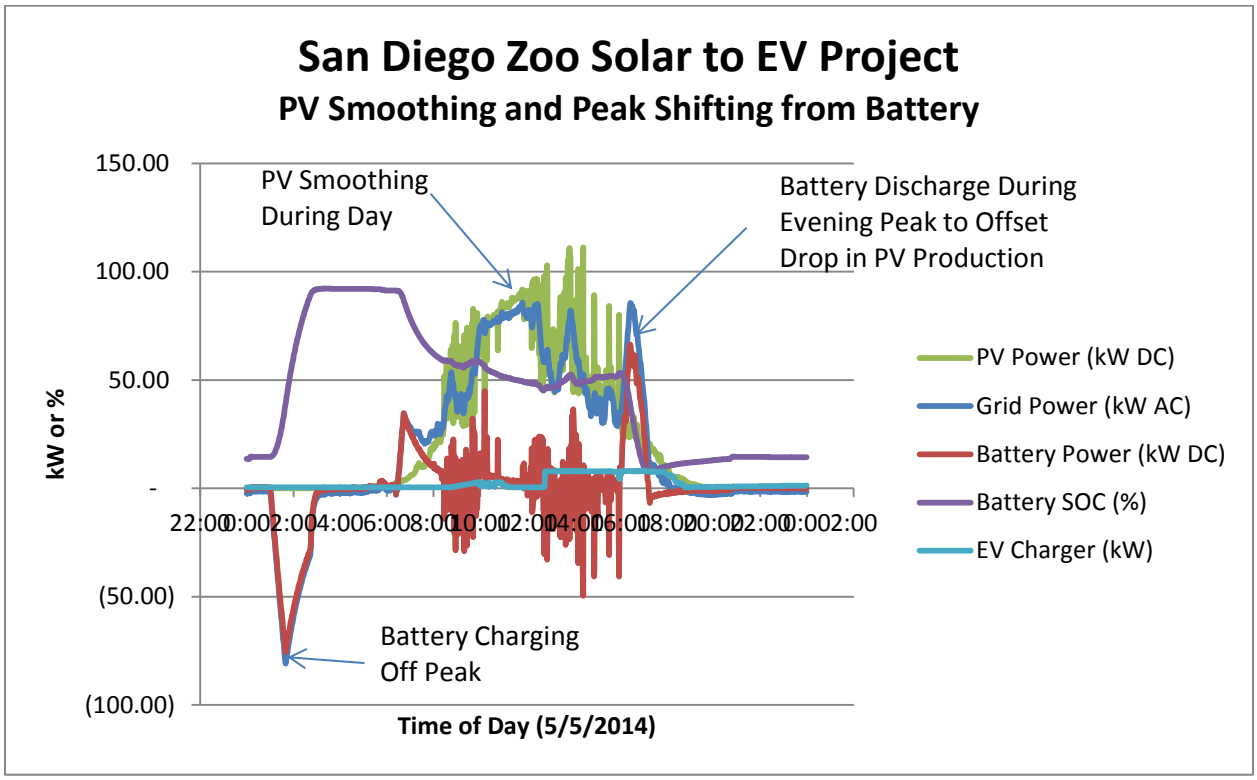

The dark red line shows the dispatch of the energy storage to counteract the intermittency of the PV (light green line). The blue line (Grid Power) shows the smoothed power output delivered to and seen by the grid.

Source: San Diego Gas and Electric Co.

3.4 Operational experience of EV Charging with solar energy

The PV solar panels at the San Diego Zoo project (Section 2.3) consist of 10 solar canopies of 9 kW each for a total PV capacity of 90 kW. During the first 9 months of operation from April to December of 2013, the PV production was up to 13,737 kWh in May of 2013. Figure 17 provides a summary of PV production from April – December, 2013. It is interesting to note that the EV charging consumes only about 15% of the PV on average, production through this time frame. With typical performance of the system, the Solar-to-EV project provides enough solar power in one day for approximately 1,500 electric vehicle miles – enough to drive from the San Diego Zoo to the St. Louis Zoo!

Table 1: PEV Energy Consumption and PV Energy Production

Month	PEV Consumption (kWh)	Zoo PV Production (kWh)	%
Nov-12*	251		
Dec-12	634		
Jan-13	180		
Feb-13	167		
Mar-13	422		
Apr-13	477	1,649	29%
May-13	673	11,056	6%
Jun-13	769	13,737	6%
Jul-13	962	12,881	7%
Aug-13	1,527	4,115	37%
Sep-13	1,388	8,089	17%
Oct-13	1,301	10,759	12%
Nov-13	1,565	6,777	23%
Dec-13	1,398	9,924	14%
Total	**11,713**	**78,987**	**15%**

The % column indicates what fraction of monthly PV production was consumed by EV charging. Issues with the inverter and associated control system resulted in several outages during the first year of operation, particularly during the months of August, September, and November.

Source: San Diego Gas & Electric Co.

The EV charging consumption followed a pattern of steadily rising monthly power consumption from a low of 167 kWh in February, 2013 to a high of 1,583 kWh in January, 2014. While EV Charging power consumption exhibited a steady increase in use during the first 8 months of operation it then leveled out at about 1,500 kWh during the second half of 2013. This increase in EV power consumption could be the result of (1) recognition, identification and adoption of the EV chargers by EV drivers, and (2) reflection of increased sales of PEVs.

It is also interesting to look at the amount of energy delivered for each individual charging episode and categorize these by kWh consumption. This provides some correlation as to what type of vehicle was charging and how often. Figure 18 shows bar figures on a monthly basis over the 13 month time frame categorized by different energy (kWh) consumption ranges: below 10 kWh, 10-19.9 kWh, 20-49.9 kWh, and greater than 50 kWh. For reference, the Nissan Leaf has a maximum capacity of about 24 kWh, the Chevy Volt 11.2 kWh, and the Tesla Model S greater than 50 kWh. The majority of charging episodes were in the less than 10 kWh range, and only less than 10 charging episodes per month used greater than 50 kWh, corresponding to a Tesla Model S' vehicle energy storage capacity.

Figure 18: Number of Plug-in Events

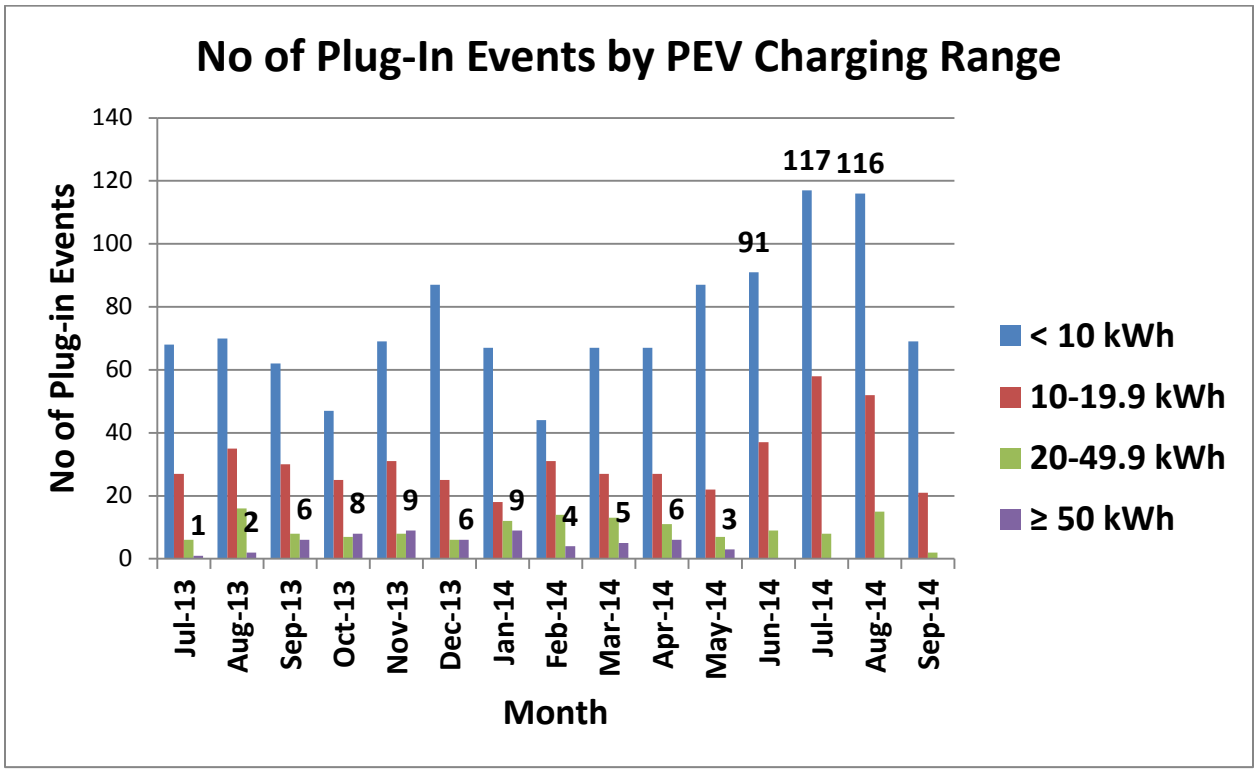

Number of monthly plug-in events categorized by EV charge consumption.

Source: San Diego Gas & Electric Co.

Examination of the load profiles for this facility provides an indication of when EV charging is most likely to occur, and correlation of this with the PV generation provides an indication of the amount of renewable energy that is being used directly for EV charging. Figure 19 shows an average of the 24 hour load profile for EV charging, for both weekdays and weekends. As expected maximum load consumption is during the weekend and mid-day hours. Peak demand is about 5 kW, and occurs during the mid-day hour from 12 noon-1 pm typically, which is when PV solar production also typically peaks. There also appears to be regular episodes of weekday nighttime charging, presumably by nearby residents who charge up for their commute.

Figure 19: Average 24 Hour Load Profile for EV Charging

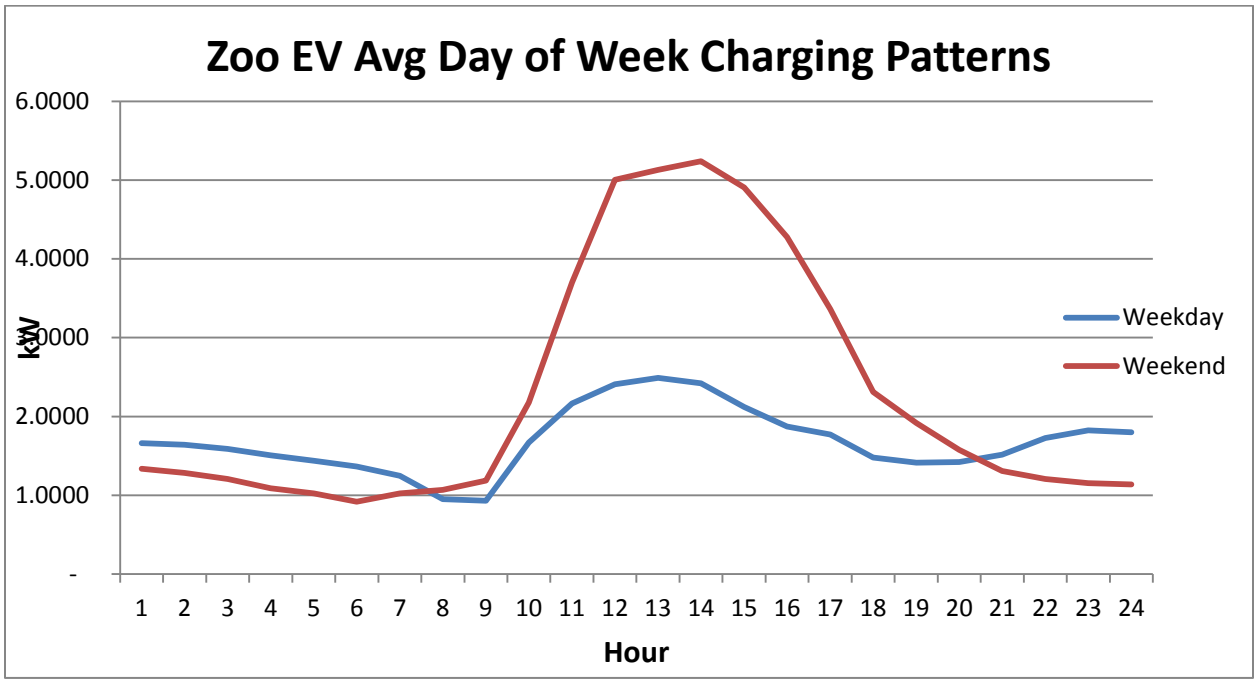

Average 24 hour load profile for EV charging for both a typical weekday and weekend.

Source: San Diego Gas & Electric Co.

3.5 Cumulative Impacts of High Penetration of EV Charging and Photovoltaic Generation

UCSD has a substantial amount of public and fleet EV level II chargers and roof top PV solar panels installed on campus. This section provides an evaluation of the impact of EV charging and PV generation on electrical distribution circuits and loads, in a microgrid setting.

There are presently 17 Blink level II EV chargers installed and operational. In addition, UCSD has installed intelligent EV charging, demonstrating the capability to have flexible pricing and automated demand response. These RWE electric vehicle charging stations are fully compatible with the global standard to be implemented in 2017 by the International Standards Organization (ISO) known as ISO 15118. At the present time 10 RWE intelligent level II EV chargers are operational.

Figure 20: RWE Intelligent Level II EV Charger

Photo Credit: UC San Diego

In addition UCSD has about 3 MW of solar roof top PV installed. Almost every campus building roof top which has sufficient structural capability has rooftop flat panel PV installed.

Figure 21: 370 kW Roof Top PV on UCSD Hopkins Parking Structure

Photo Credit: UC San Diego

UCSD has several data collection systems. Most of the data is consolidated in the OSI Soft PI data process book, but data is also available directly from individual devices. This allows collection of higher resolution data, if necessary. Data examined included EV charging session data, which was available from Blink and KnGrid which are managing the Blink EV chargers and the RWE intelligent chargers, respectively. This EV charging session data includes the start and end times of charging events as well as the amount of energy (kWh) consumed during the

charge session. Distribution system voltages were monitored at the 480 V AC panel where the EV chargers are connected. This data was available through monitoring ION 7550 smart meters located at each panel. In addition some PV power production data was available. The analysis included correlation of events for EV charging and PV power production and voltage measurements.

Since the low granularity of the available voltage data did not allow examination of voltage impacts at the exact time when the charge event started, the project team hypothesized that the impact of EV charging should manifest in a decrease in the minimum voltage recorded during the 15 minute interval including the charge event compared to the previous interval. However, Figure 22shows, for one meter with two EV charging stations, that there is no difference in the voltages. Therefore, no impacts of EV charging on distribution system voltages was determined.

Figure 22: Minimum Voltage Deviations for the Preceding and Coinciding Intervals

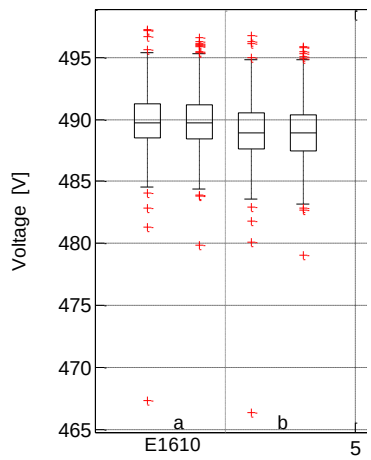

For each phase (a, b) the distribution of voltage data for the preceding interval is shown at left and for the coinciding interval at right.

Similarly, impacts of PV variability were examined during partly cloudy conditions relative to clear periods. The range between minimum and maximum voltage over a 15 minute interval on meters near PV systems was not found to be statistically different than the range during the preceding clear interval. Therefore, no impacts of PV variability on voltage were detected.

In summary, the results of this analysis included the following key findings:

- No significant voltage drop due to EV charging.
- Building load variations generally exceeded the impact of EV charging load variation.
- No significant adverse impact of PV power production on voltage deviation was observed. However, additional voltage monitoring of distribution circuits is needed.

3.6 Solar Forecast Results

3.6.1 Forecasting Using Ground Data without Sky Imagery

Figure 23 shows the distribution of the length of the maximum forecast horizon when the initial power distribution has been completely advected out of the plant footprint. The median of the possible forecast horizon is 54 s which corresponds to cloud speeds of 33.5 and 9.9 m s-1 for the longer and shorter dimension of the power plant, respectively. Furthermore, the forecast horizon of 180 s covers the complete advection of the initial grid 95.4% of the time. Since the applicable forecast horizon is a function of local cloud speed meteorology and plant dimensions, it is expected to vary strongly site-by-site. Table 2 shows the rRMSE of the forecast methods that do not require sky images. As expected, the cloud speed persistence forecast outperforms persistence throughout the 180 s time horizon. The simpler approach of ramp persistence provides the best forecast results for the first 32 s of forecast horizon with forecast skills up to 45%.

Table 2: The rRMSE of the Forecast Methods that Do Not Require Sky Images

horizon	20 s			60 s			120 s		
	P	r skill	csp skill	p	r skill	csp skill	p	r skill	csp skill
%	3.3	23.4	12.1	8.2	-25.5	7.2	12.7	-60.1	2.6

rRMSE of persistence (p) and forecast skill (Eq. 6) of ramp (r) and cloud speed persistence (csp) compared to the rRMSE of persistence at different forecast horizons

Figure 23: Distribution of the Length of the Maximum Forecast Horizon

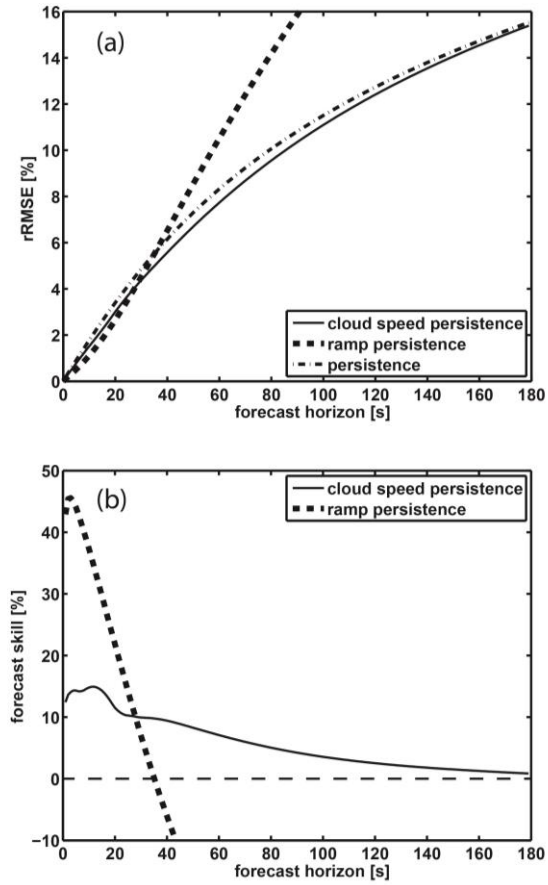

a) rRMSE [%] of cloud speed persistence, ramp persistence, and persistence as a function of forecast horizon. b) Forecast skills for ramp and cloud speed persistence over persistence.[13]

[13] Lipperheide, M., JL Bosch, J Kleissl. Embedded nowcasting method using cloud speed persistence for a photovoltaic power plant, *Solar Energy*, doi:10.1016/j.solener.2014.11.013, 112: 232–238, 2015.

Figure 23: Distribution of Maximum Forecast Horizons

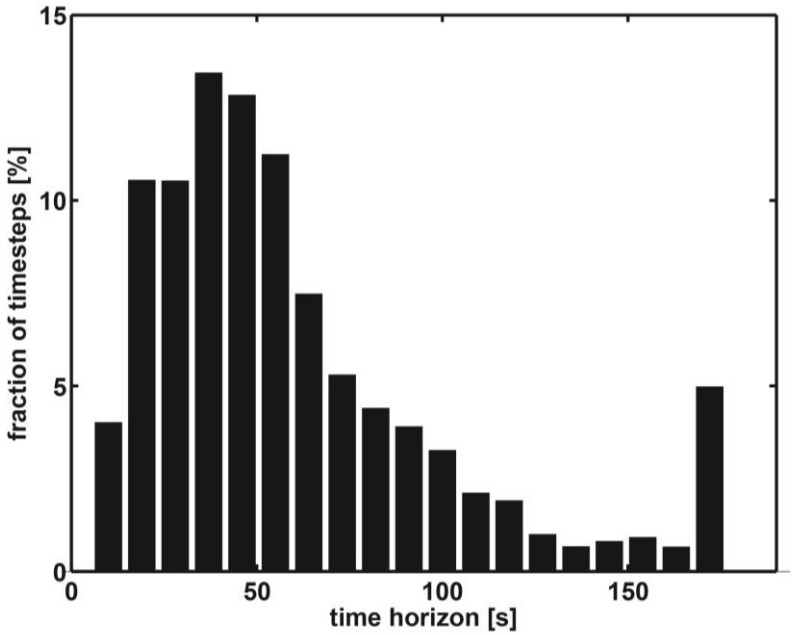

Distribution of maximum forecast horizons for which cloud speed persistence can be applied without extension by delayed persistence. The value at 180 s is cumulative for 180 s and greater.

3.6.2 Sky Imagery Forecast Results

The results presented here are for the week of November 9-15, 2011 which provided a variety of conditions with clear, partly cloudy, and overcast days. Forecast performance as a function of forecast horizon is shown in Figure 24a. The forecast error of persistence steadily increases, whereas the forecast error of the sky imager starts off at a larger value due to shadowband issues and cloud decision errors near the sun, and then levels off after about 3-4 minutes. The shadowband can block out the entire sky region over the plant that contains the clouds that are causing the irradiance impact (Figure 24), and as a result minimal or no data to generate a forecast is available. As the shadowband is 'advected' away at longer forecast horizons, valid data from another part of the image moves to the region of sky over the plant in the path of the sun and a more accurate forecast results.

Figure 24: Forecast Performance

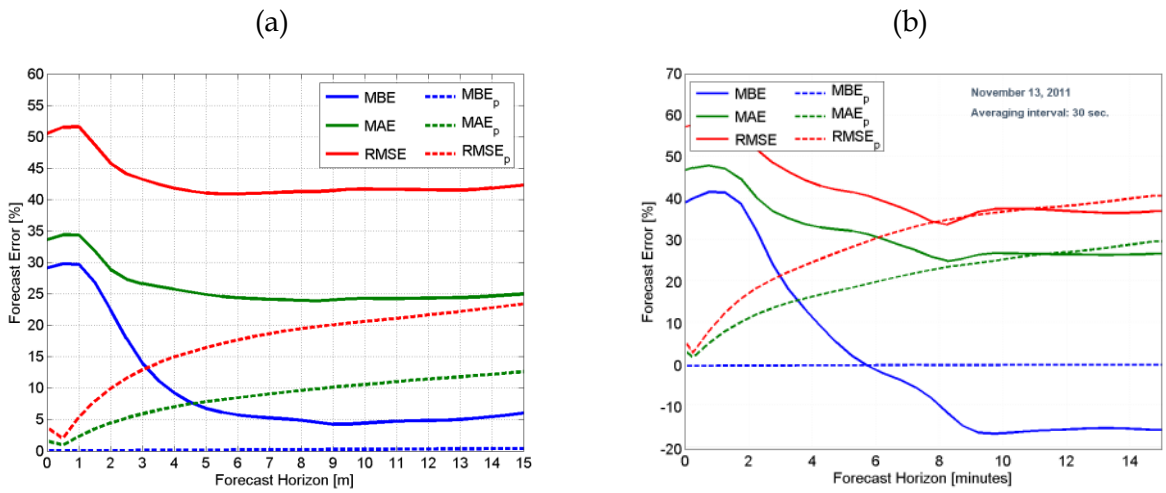

Forecast performance as a function of horizon for a sky imager forecast (solid) and persistence (dashed) shown for (a) November 9th - 15th, 2011, and (b) November 13th, 2011 only.

The mean absolute forecast error for the 5, 10 and 15 minute forecast horizons are presented for each day individually, and for the 1 week period in Table 3. Considering individual days provides performance information on different cloud regimes. On clear days the sky imager adds little value, a fact which is obvious since its purpose is to image and track clouds. On clear days the sky imager forecast error is nonzero due to small errors in the modal clear value. Persistence uses a recent average of normalized power which is more accurate than the most frequent daily value (i.e. the mode) when the input solar signal is not impacted by clouds.

The storm on November 11th brought very optically thick clouds which caused an error in the cloud decision step erroneously yielding clear sky forecasts. This issue has been addressed in new cloud decision research[14]. As a result of the poor cloud decision, the forecast error was very large on this day.

[14] Ghonima M, Urquhart B, Chow CW, Shields JE, Cazorla A, and Kleissl J (2012). A method for cloud detection and opacity classification based on ground based sky imagery. Atmospheric Measurement Techniques, Volume 5, pp. 4535-4569, doi:10.5194/amtd-5-4535-2012.

Figure 25: Cloud Overlay from the Total Sky Imager Over the Copper Mountain Solar Power Plant

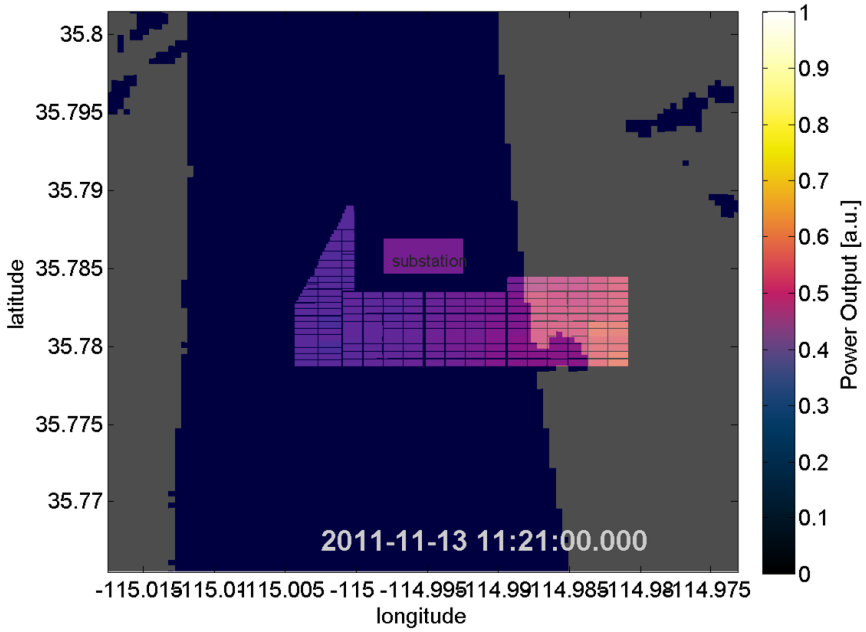

Cloud overlay from the total sky imager over the Copper Mountain solar power plant on November 13th, 2011. The projection of the shadowband covers about 2/3 of the power plant.

When there are clouds, the sky imager adds value because it can forecast when a ramp will occur, and it can provide a reasonable approximation of the magnitude. Partly cloudy days with significant ramping occurred on the 10th, 12th, and 13th. The error on the 13th is shown as a function or forecast horizon in Figure 24b. Due to frequent ramping, the persistence forecast error increases significantly after a few minutes, and the sky imager performs better.

The performance results here show the accuracy of the current state-of-the-art deterministic forecast. In an operational setting, this forecast will be adjusted to use persistence for clear days, thus rendering the results on November 9th, 14th, and 15th less meaningful. Only the remaining days should be considered as true indicators of how the current forecast methods perform. The results on the 11th reported high cloud fraction, but small plant shading fraction was observed, indicating nearly all the large error was due to the cloud detection reporting clear skies near the sun. This is a serious but correctable issue, and due to the overcast nature of this day, results are likely to be similar to or more accurate than the remaining cloudy days. The remaining three days (10th, 12, and 13th) provide the most representative accounting for the current status of the sky imager forecasts. Many of the errors here beyond the 5 minute forecast horizon (which is plagued by the shadowband) are attributable to geometric errors in the pseudo-cartesian transformation. The causes are both the geometric calibration of the instrument, and the flat cloud field assumption. Higher accuracy geometric calibration procedures are being applied to new instrumentation, and new algorithm development is underway to move from the 2D cloud field assumption, to construction of the cloud field in 3D.

Table 3: Sky Imager (SI) and Persistence (P) Forecast Error

	5 min.		10 min.		15 min.	
	SI	P	SI	P	SI	P
9[c]	4.5	0.9	5	1.3	5.1	1.7
10	42.6	14.9	39	18.5	42	22.1
11	152.7	8	161.8	13.9	157.7	18.6
12	33.9	23.2	33.6	30.7	38.8	35.6
13	32	17.5	26.5	24.7	26.4	29.3
14[c]	4.9	1.5	4.2	1.9	4.1	2.2
15[c]	6.7	1.3	6.7	1.8	6.7	2
1 week	24.9	7.8	24.3	10.6	25	12.6

Sky imager (SI) and persistence (P) forecast error at selected time horizons of 5, 10 and 15 minutes. Error is given as mean absolute error. Error is reported for individual days and the aggregate set of days as a percentage of average power generated during daylight hours. The c superscript indicates the day was clear.

The ability for a sky imager to capture ramps is illustrated in Figure 26 for the 10 minute forecast horizon. Constant values in the sky imager forecast indicate periods when the plant is forecast to be entirely clear or entirely cloudy. Temporal shifting of ramp forecasts versus actual ramps can be seen, in both the early or late directions. Ramps are also missed and falsely predicted. The ramp forecast is directly related to how well the shadows predicted by the sky imager match plant observations. Ramp timing errors are caused by any combination of inaccurate cloud decision, camera resolution, geometric calibration errors, cloud advection errors, and differences in cloud morphology due to viewing angle. Because of the novelty of the system, each error source described can be improved markedly and thus the overall ramp forecast performance is expected to improve.

Figure 26: Midday 10 Minute Forecast Performance

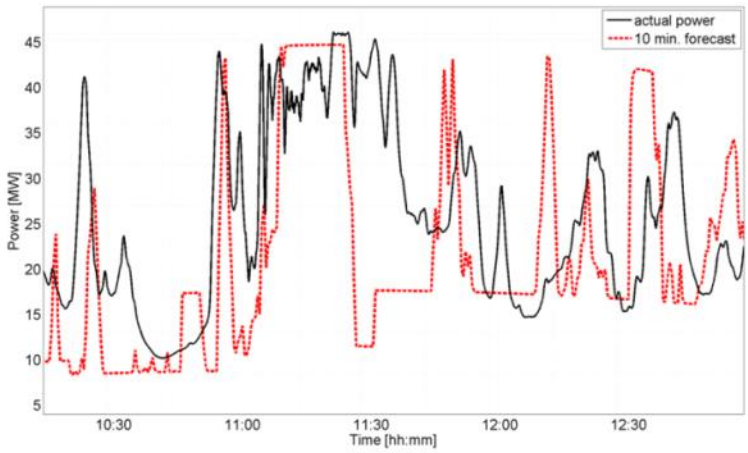

Midday 10 minute forecast performance on November 13th, 2011 showing how the sky imager captures ramps at 10 minutes in the future. A perfect forecast would have both curves matching exactly.

CHAPTER 4:
Distributed Energy Resource Characterization and Lessons Learned

4.1 Battery Degradation and Life Expectancy

The management of the individual batteries and modules is important to ensuring long battery life for long endurance energy stationary energy storage applications. The Sanyo DESS battery management control unit (BMU) was designed to monitor and calculate in real time the voltage and temperature of each individual lithium-ion battery cell and make adjustments to optimize performance. Based on continually monitoring voltage, current and temperature data from the individual cells the control system estimates the life span of each cell and optimizes the performance of the battery system. In addition a Power Management Unit (PMU) manages the discharge and charge rates of the overall battery system. The main purpose of the PMU is to ensure that the DESS operates within safe limitations, and acts mainly as protection functions.

Through the BMU and PMU, the DESS was operated as follows: Each day two cycles of Charge and Discharge between 30% and 80% of State of Charge (SOC). For all times the charging by discharging stops at either the programmed end time or when the system reached 80% by 30% SOC, whichever is earlier:

a. 8am - 12 noon : 5kW continuous Charge

b. 12 noon - 3:30pm : 4kW continuous Discharge

c. 3:30pm - 7 pm : 6kW continuous Charge

d. 7pm - 10:20pm : 5kW continuous Discharge

e. 10:20pm – 8 am: No operation and stay at SOC 30%

Normally, as the battery begins to degrade, the amount of discharged energy gets smaller. The amount of discharged energy in each 10 minute interval is calculated from the data of input current and voltage during each interval. The total amount of discharged energy at each cycle from 80% to 30% is summed. Observing the change of this total amount through the entire experiment provides the kWh capacity equivalent of 50% SOC, indicating the degradation of the useable capacity of the battery.

This limited amount of performance data analysis indicates that for two cycles per day under 50% Depth of Discharge (DOD) the estimated lifecycle to reach 60% of the initial capacity is 366 days. However, we deem the analysis inaccurate as after quality control only a few charge cycles could be used to obtain this result. This estimated lifecycle (366 days, 1 year) is too short from based on our knowledge and experience. The following is an estimation of life expectancy based on lab tests performed on the batteries and is provided for reference.

Lifecycle lab test result and analysis are based on the same battery pack used at UCSD under the same condition as much as possible. Batteries are charged and discharged twice per day between 30 to 80% SOC at a discharge rate of 0.15C. The batteries remain at SOC 100% for 9.7 hours. The temperature was held steady at 25oC.

Figure 27: Degradation of Battery Capacity During Laboratory Tests

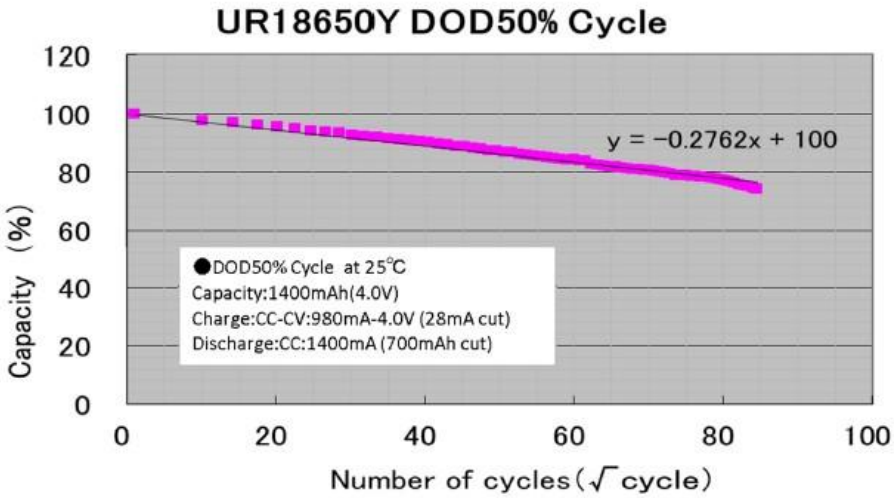

Source: Sanyo/ Panasonic Corp.

The lab test condition represented 5 years corresponding to 3650 cycles (= 2 cycles per day x 365 days x 5 years) of continuous operation. For these lab tests, degradation by cycles was 16.7% and degradation by storage was 8.3% after 5 years. The 5 year total degradation was 25.0% meaning that the capacity would be at 75% of the initial capacity after 5 years. The UCSD degradation would be expected to even smaller as non-operation (1020pm to 8am) occurred at 30% SOC versus 100% SOC in the lab tests. Therefore, based on lab test conditions, the estimated life expectancy to reach 60% capacity would be about 15 years. At that time the degradation by cycles would be 28.9% and degradation by storage would be 14.4%. It is expected that about 60% of the battery capacity would remain after 15 years, if the batteries were cycled based on the same duty cycle used in the UCSD application.

4.2 Battery System Charge Efficiency

The system operation was monitored during charge and discharge cycles, and the input and output power was measured after each major component. From these measurements the overall system efficiency and the efficiency of each component were determined. Figure 28 shows a summary of the efficiency of the entire Lithium Ion Battery (LIB) energy storage system and the Power Conditioning System (PCS).

Figure 28. Sanyo-Panasonic Energy Storage System Efficiency

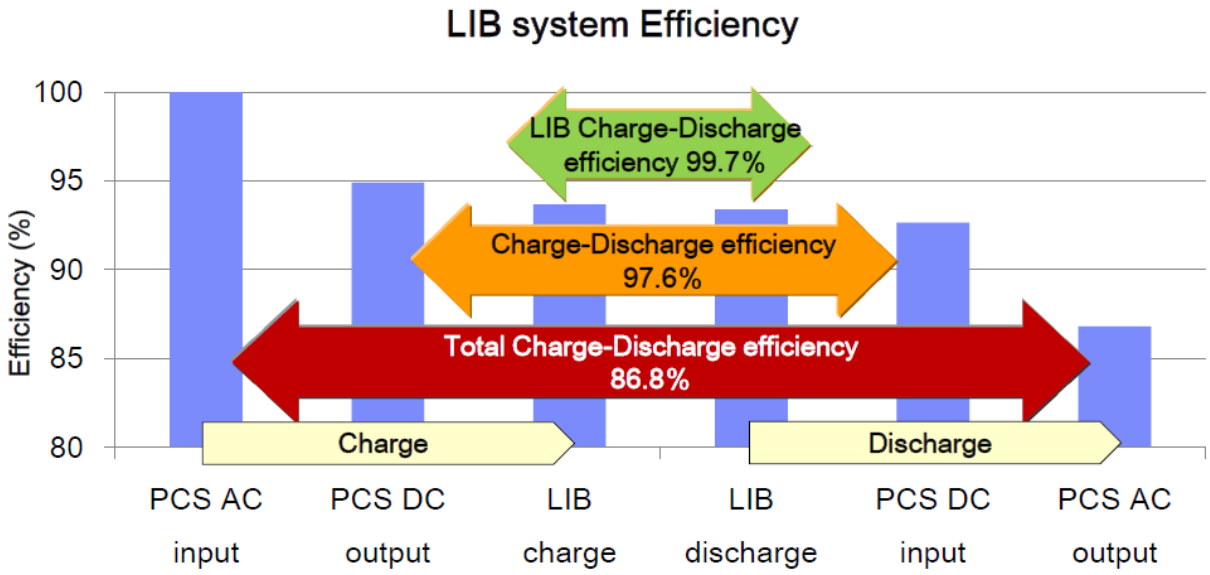

Source: Sanyo / Panasonic Corp.

4.3 EV Charging Costs and CO2 Emissions

PV Solar EV charging offers a clean source of energy for charging electric vehicles, and when coupled with energy storage, it also provides a reliable source of power. However the question of cost effectiveness of PV solar EV charging is an issue that needs to be examined. As a measure of potential cost effectiveness the cost of PV Power Purchase Agreement (PPA) costs is compared to the CPUC approved EV charging experimental rates that were established for the SDG&E service territory. The average cost of UCSD PPA is currently $ 0.185 per kWh.

San Diego Gas & Electric Company (SDG&E) conducted a multi-year plug-in electric vehicle (EV)1 Pricing and Technology Study (Study), incorporating a temporary experimental EV rate approved by the California Public Utilities Commission (CPUC). SDG&E EV customer participants were randomly assigned to one of three EV tariffs, each with different price ratios between on-peak, off-peak and super off-peak rates.

When examining off-peak and super off-peak periods it appears that rates are lower than the $ 0.185 per kWh for PV solar PPAs at UCSD. The off-peak EV charging rates range from a low of $ 0.14 per kWh and to a high of $ 0.17 per kWh. The super off-peak period EV charging rates range from a low of $ 0.06 per kWh to a high of $ 0.14 per kWh. However, both of these periods are during night-time hours and really have no application to PV solar, without energy storage.

During on-peak hours the EV charging rates are generally much higher than the $ 0.185 per kWh PV PPA rate paid by UCSD for PV solar production. The EV charging rates for on-peak hours ranges from a low of $ 0.16 per kWh to a high of $ 0.36 per kWh.

Another comparison is the time of use rates (EV-TOU2 Whole House rate) currently offered outside of the EV experimental rate program. This EV charging rate, shown in Figure 29, is

clearly more expensive than the PV PPA UCSD average rate during the day light hours for both On-peak and Off-peak periods.

Figure 29: SDG&E EV-TOU2 Whole House Rate

(Ref. SDG&E EV TOU Postcard, September 1, 2013)

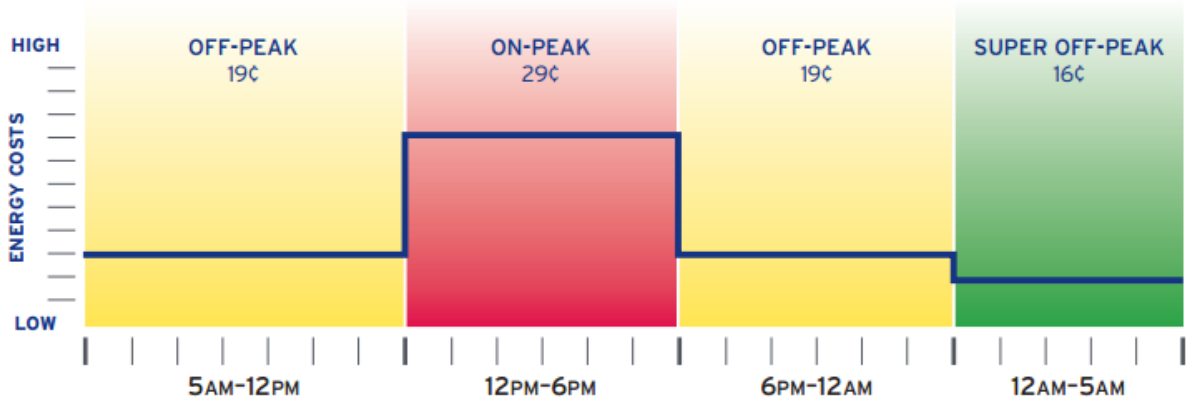

Source: San Diego Gas & Electric Co.

This cost analysis only gives an approximate cost comparison, it is not considered to be an exhaustive valuation of Renewable EV charging and a comparison to EV charging rates. The average UCSD PPA rate may not reflect average PPA rate throughout California, also the average PPA rate may not include all of the balance of plant costs that would be required for a Renewable EV Charging including EV charging facilities and energy storage. Also the EV Charging rates discussed here are the SDG&E EV Time of Use (TOU) rates that would apply to residential customers for EV charging. Other EVSE vendors actually charge higher rates, for example Blink EV charging currently charges $ 0.49 per kWh.

Regarding CO2 emissions, the California Air Resources Board (CARB) has established the CA generation mix at 446 g of CO2 per kWh for the average CA electricity mix and 377 g of CO2/kWh for the marginal generation mix [CARB, 2011]. The UCSD microgrid in 2012 generation mix was estimated to be 266 g of C02 per kWh, or 29% lower than the CA marginal generation mix, due to the CHP & commissioning of a 2.8 MW base load, directed biogas fuel cell on campus. With an assumed Smart EV efficiency of 0.2 kWh per mile fueled from the UCSD's microgrid in 2012 was expected to achieve a well-to-wheel emission characteristics of 51 g of CO2 per mile. Using the lower carbon emitting generation from the UCSD microgrid, the 51 g of CO2 per mile represents a 79% improvement over the U.S. EPA and NHTSA standards required of major OEMs to meet an estimated combined average emissions level of 250 grams of CO2 per mile by 2015 [CEC, 2011].

4.4 Intra-Hour Solar Forecast Accuracy

Encouraging results are obtained from a cloud speed persistence method applied to spatially resolved inverter power output for a large utility-scale solar power plant. While the forecast horizon is short due to high cloud speed at this site, the new method performs better than the baseline persistence approach, especially within the first minute of forecast. However, the ramp

persistence method shows better forecast results for the first 32 s. Nevertheless, cloud speed persistence is a consistently skillful nowcast approach with a rRMSE of 2.9% at 20 s and 7.6% at 60 s, outperforming persistence by 12.1% and 7.2% at these forecast horizons. We are not aware of previous published studies on very short-term forecasting using solely endogenous data. However, Pedro & Coimbra[15] demonstrated forecast skill of 32.2% for 1 hour-ahead forecasts using endogenous data. Using a similar cloud speed persistence approach applied to spatially distributed PV power output data (but with a much larger average spacing of 3 km) Lonij et al.[16] achieved forecast skills of -4.6% and 2.4% for 15 and 30 min forecast horizons, respectively. Chu et al.[17] showed that for a 5 min forecast horizon a forecast skill of up to 20.9% can be achieved using exogenous sky imagery. The cloud speed persistence method is associated with smaller forecast skill, but for the very short forecast horizon, persistence is more competitive and only endogenous data is used.

The performance results for the selected week indicate that more work is required to make sky imagery based short-term forecasting a viable technique. The key finding in this study is that the TSI as an instrument is not suitable for generating short-term solar power forecasts. The reasons for this are: a) the shadowband eliminates important sky data for forecasting *and* its presence makes assessment of forecast errors due to geometry more challenging (i.e. it makes research on forecast improvement more difficult); b) low resolution imagery that is jpg compressed, further reducing information content, c) cloud decision errors near the sun and the horizon.

The MBE, MAE, and RMSE error metrics are truly gross statistics and do not fully characterized all aspects of forecast performance. These metrics indicate that, overall, persistence performs much better than the sky imager. When interpreting the performance results provided by these metrics it is important to remember that they do not capture the ability of the system to capture ramp events. These metrics measure only the typical difference between the forecasts and the actual power produced. For instance, during a clear period persistence will provide a smaller forecast errors than the algorithm presented, but it will never predict a ramp from an oncoming cloud. Ramp forecasting metrics are being developed to quantify the sky imager's performance.

To eliminate shadowband and resolution issues, the Kleissl group has built an advanced sky imager (named USI) that will eventually be installed at Copper Mountain to help further forecasting development. The USI has since been deployed at over 10 sites in California and nationwide. Improved instrumentation together with improved cloud decision algorithms and integration of sky imager forecasts with stochastic learning techniques are believed to ultimately yield to unprecedented forecast accuracy for 1 to 15 minute forecast horizons.

---

[15] Pedro, H. T., & Coimbra, C. F. (2012). Assessment of forecasting techniques for solar power production with no exogenous inputs. *Solar Energy , 86*, 2017-2028.

[16] Lonij, V. P., Brooks, A. E., Cronin, A. D., Leuthold, M., & Koch, K. (2013). Intra-hour forecasts of solar power production using measurements from a network of irradiance sensors. *Solar Energy , 97*, 58-66.

[17] Chu, Y., Pedro, H. T., & Coimbra, C. F. (2013). Hybrid intra-hour DNI forecasts with sky image processing enhanced by stochastic learning. *Solar Energy , 98*, 592-603.

CHAPTER 5:
Summary and Conclusions

UCSD has conducted long term field testing of Distributed Energy Storage Systems over three years. The DESS tested included both new lithium-ion batteries and used PEV batteries. There were some notable challenges, since electrical and safety standards for this type of energy storage system had not been fully developed, but valuable performance information has been gained. Energy storage based on lithium ion batteries appears to be highly efficient. However, the balance of plant including the Power Conditioning System (PCS) can result in a significant reduction in overall system efficiency. In this project for a lithium-ion battery system, the balance of plant reduced efficiency from 99.7% to about 88.6%. Battery life expectancy will be highly dependent on the use case application used for the DESS. Cycle life expectancy will be less for applications involving higher depth of discharge (DOD), such as peak load reduction. Correspondingly, cycle life expectancy will be longer for DESS applications that involve small DOD, such as frequency regulation or Regulation Energy Management.

When integrated directly with PV, energy storage can enhance the overall performance of renewable generation, make it more dispatchable, and reduce the impacts of variability. In addition, energy storage can provide ancillary services such as frequency regulation, as demonstrated in this project. Energy storage is also a key element to minimizing the impact of periodic EV charging demands. The following energy storage use cases were demonstrated:

- Smoothing of renewable intermittency
- Peak Load Reduction using stored solar PV generation
- Energy Arbitrage
- Demand Charge Management
- Regulation Energy Management

It has been shown that energy storage can provide support to the grid by storing PV generation during the middle of the day and discharging during the peak load period in the late afternoon and early evening. Energy storage can also provide voltage and frequency regulation and other ancillary services that can support the local distribution grid. More work is needed to develop control algorithms that will optimize the operation and use of systems which couple PV production and EV charging. These new control algorithms could conceivably incorporate EV charging price signals that will reflect periods when local solar production is high and periods when power grid demand is high and solar production is low. UCSD's smart charging project with RWE is one such example of this type of EV charging price signal that will reflect local demand, weather forecasting, customer- and fleet-defined requirements and utility engagement.

The renewable EV charging project implemented by the San Diego Smart Cities team has demonstrated a viable and sustainable approach for providing reliable clean transportation. The estimated reduction in carbon footprint provide by this project is equivalent to removing 189,216 pounds of CO2 from the atmosphere or removing 21 cars from the road each year. With correct implementation, the combination of energy storage, PV, and EV charging can be

coordinated to reduce detrimental impacts to the operation of the grid, and provide support to the grid when needed. It was observed that it took 6-8 months for EV users to begin to use the charging stations on a regular basis.

The CAISO has had access to the UCSD real time operations and behind the meter resources through Power Analytic's Paladin system, and has gained valuable insight and information on how microgrids operate and how they may participate as resources in the future. The ability to control behind the meter energy resources on the microgrid and the integration of real-time analytics of the microgrid were essential to the analysis of energy information and UCSD's ability to respond to DR requests. The results of the market simulation did provide a number of data points supporting basic market familiarity and the potential of market participation. The regulation test of the UCSD NGR resource was completed successfully when it ran on a simulated AGC signal and showed similar patterns as other AGC scenarios observed in previous market simulations.

GLOSSARY

Acronym/Term	Meaning
AGC	Automatic Generation Control
CAISO	California Independent System Operator
CAM	Commission Agreement Manager
CAO	Commission Agreement Officer
CPR	Critical Project Review
CPUC	California Public Utilities Commission
DESS	Distributed Energy Storage Systems
DER	Distributed Energy Resources
DOD	Depth of Discharge
EV	Electric Vehicle
GHI	Global Horizontal Incident Solar Irradiance
IOU	Investor-Owned Utility
NGR	Non Generator Resource
NSRDB	National Solar Radiation Database
NWP	Nation Weather Prediction
PAC	Project Advisory Committee
PDR	*Proxy Demand Resource*
PV	Photovoltaic
RE	Renewable Energy
RTO/ISO	Regional Transmission Operator/Independent System Operator
TAC	Technical Advisory Committee
T&D	Transmission & Distribution
TSI	Total Sky Imager
UCSD	University of California, San Diego

REFERENCES

Bosch, Juan Luis, and Jan Kleissl. "Cloud motion vectors from a network of ground sensors in a solar power plant." *Solar Energy* 95 (2013): 13-20.

Chow, Chi Wai, et al. "Intra-hour forecasting with a total sky imager at the UC San Diego solar energy testbed." *Solar Energy* 85 (2011): 2881-2893.

Chu, Yinghao, Hugo T.C. Pedro, and Carlos F.M. Coimbra. "Hybrid intra-hour DNI forecasts with sky image processing enhanced by stochastic learning." *Solar Energy* 98 (2013): 592-603.

Coimbra, Carlos F.M., Jan Kleissl, and Ricardo Marquez. "Chapter 8 - Overview of Solar-Forecasting Methods and a Metric for Accuracy Evaluation." In *Solar Energy Forecasting and Resource Assessment*, edited by Jan Kleissl, 171-194. Boston: Academic Press, 2013.

Dong, Zibo, Dazhi Yang, Thomas Reindl, and Wilfred M. Walsh. "Short-term solar irradiance forecasting using exponential smoothing state space model." *Energy* 55, no. 0 (2013): 1104-1113.

First Solar. "Copper Mountain Solar 1 Datasheet." *Available through: http://www.firstsolar.com/Projects/Copper-Mountain-Solar-1 (Accessed 23 May 2013)*, 2011.

Fung, Victor, Juan Luis Bosch, Steve W. Roberts, and Jan Kleissl. "Cloud speed sensor." *Atmospheric Measurement Techniques Discussions* 6 (2013): 9037-9059.

Google Maps. "PV Plant at Henderson (NV) 35°47'00.06"N, 114°59'33.10"W, elevation 564 m." 2013.

Hill, Cody A., Matthew Clayton Such, Dongmei Chen, Juan Gonzalez, and W. Mack Grady. "Battery Energy Storage for Enabling Integration of Distributed Solar Power Generation." *IEEE Transactions on Smart Grid* 3 (2012): 850-857.

Hoff, Thomas E., and Richard Perez. "{Quantifying PV power Output Variability}." *Solar Energy* 84 (2010): 1782-1793.

Ineichen, Pierre, and Richard Perez. "A new airmass independent formulation for the Linke turbidity coefficient." *Solar Energy* 73, no. 3 (2002): 151-157.

Inman, Rich H., Hugo T.C. Pedro, and Carlos F.M. Coimbra. "Solar forecasting methods for renewable energy integration." *Progress in Energy and Combustion Science* 39, no. 6 (2013): 535-576.

Lave, Matthew, Jan Kleissl, and Joshua Stein. "{Chapter 7 - Quantifying and Simulating Solar-Plant Variability Using Irradiance Data}." In *Solar Energy Forecasting and Resource Assessment* , edited by Jan Kleissl, 149-169. Boston: Academic Press, 2013.

Lonij, Vincent P.A., Adria E. Brooks, Alexander D. Cronin, Michael Leuthold, and Kevin Koch. "Intra-hour forecasts of solar power production using measurements from a network of irradiance sensors." *Solar Energy* 97 (2013): 58-66.

Mammoli, A., A. Menicucci, T. Caudell, A. Ellis, S. Willard, and J. Simmins. "Low-cost solar micro-forecasts for PV smoothing." 2013. 238-243.

Marquez, Ricardo, Hugo T.C. Pedro, and Carlos F.M. Coimbra. "Hybrid solar forecasting method uses satellite imaging and ground telemetry as inputs to ANNs." *Solar Energy* 92, no. 0 (2013): 176-188.

Mills, Andrew D., and Ryan H. Wiser. "Changes in the Economic Value of Variable Generation at High Penetration Levels: A Pilot Case Study of California." 06/2012 2012.

Page, John. "1 - The Role of Solar Radiation Climatology in the Design of Photovoltaic Systems." In *Practical Handbook of Photovoltaics*, edited by Tom Markvart and Luis CastaÃ±er, 5-66. Amsterdam: Elsevier Science, 2003.

Pedro, Hugo T.C., and Carlos F.M. Coimbra. "Assessment of forecasting techniques for solar power production with no exogenous inputs." *Solar Energy* 86 (2012): 2017-2028.

Perez, Richard, and Tom E. Hoff. "Chapter 10 - SolarAnywhere Forecasting." In *Solar Energy Forecasting and Resource Assessment*, edited by Jan Kleissl, 233-265. Boston: Academic Press, 2013.

Perez, Richard, et al. "A new operational model for satellite-derived irradiances: description and validation." *Solar Energy* 73, no. 5 (2002): 307-317.

Perez, Richard, Sergey Kivalov, James Schlemmer, Karl Hemker Jr., David Renné, and Thomas E. Hoff. "{Validation of short and medium term operational solar radiation forecasts in the US}." *Solar Energy* 84 (2010): 2161-2172.

Sherwood, Larry. "{U.S. Solar Market Trends}." *Interstate Renewable Energy Council (IREC)*, 2013.

Solarwirtschaft. "{Statistische Zahlen der deutschen Solarstrombranche}." *Available through: http://www.solarwirtschaft.de/fileadmin/media/pdf/bsw_solar_fakten_pv.pdf (Acessed 10 January 2014)*, 2014.

Yang, Handa, et al. "Solar irradiance forecasting using a ground-based sky imager developed at UC San Diego, accepted with minor revisions in Solar Energy." 2014.